THE KINETIC AND THERMODYNAMIC PROPERTIES OF THE DISSOLUTION OF SODIUM BISMUTHATE

A Thesis

by

ANDREW JOHN WILCOX

Submitted to the Office of Graduate and Professional Studies of
Texas A&M University
in partial fulfillment of the requirements for the degree of

MASTER OF SCIENCE

Chair of Committee,	Sunil S. Chirayath
Co-Chair of Committee,	Jonathan D. Burns
Committee Members,	Charles M. Folden III
Head of Department,	Yassin A. Hassan

May 2018

Major Subject: Nuclear Engineering

ABSTRACT

The development of a group actinide separation of U, Pu, Np, and Am could significantly simplify the closure of the nuclear fuel cycle, while reducing the amount of nuclear waste produced. To perform this group extraction the difficult separation of Am^{3+} from Cm^{3+} and the trivalent lanthanides must be addressed. Higher oxidation states of Am have been observed but require a high oxidizing potential to achieve. $NaBiO_3$ has been shown to be capable of oxidation of Am(III)/Am(VI) in highly concentrated nitric acid and is known to be a cost effective and easily produced oxidizing agent. The slow dissolution kinetics of sodium bismuthate that have been observed, as well as its low solubility in nitric acid, represent some concerns in adoption of a process in which it is implemented. For this reason a thorough investigation of these properties as a function of nitric acid concentrations was undertaken. In addition, the effect of having other metal ions present in solution, like Cs^{+}, Sr^{2+}, Nd^{3+}, Zr^{4+}, $Ce^{3+/4+}$, or UO_2^{2+} on the dissolution behavior of sodium bismuthate was determined. Except in the case of Sr^{2+} these metal ions were seen to reduce the solubility limit of sodium bismuthate to varying degrees, while each ion was also found to either have a neutral or positive effect on the dissolution rate.

DEDICATION

To my family and close friends who gave me endless support and words of encouragement throughout my life. Without all of you I am sure I would not be the person I am today.

ACKNOWLEDGEMENTS

I would like to thank my committee co-chair, Dr. Burns, for his continued patience and guidance throughout the course of this research. You have been a great advisor, imparted knowledge and wisdom to me, and helped me to learn from my mistakes in a positive way. Not only have you provided direction in aspects related to this work but for life in general. Without you this thesis would not have been possible.

I would also like to thank co-chair Dr. Chirayath for being an excellent teacher and to my other committee member Dr. Folden for their guidance and support throughout the course of this research.

I would like to thank Dr. Kitcher, Dr. Tomlin, and Dr. Ortega for their assistance in completing my thesis

Thanks also go to my friends and colleagues and the department faculty and staff for making my time at Texas A&M University a great experience.

CONTRIBUTORS AND FUNDING SOURCES

Contributors

This work was supervised by a thesis committee consisting of Dr. Jonathan D. Burns [co-advisor], and Dr. Sunil S. Chirayath [co-advisor] of the Nuclear Engineering Department and Dr. Charles M. Folden III of the Department of Chemistry.

All work for the thesis was completed by the student, in collaboration with Vedant Sureja of the Department of Economics.

Funding Sources

This work was sponsored by The Fuel Cycle Research and Development program, Office of Nuclear Energy, U.S. Department of Energy.

This work was also sponsored by The Nuclear Energy University Program, Office of Nuclear Energy, U.S. Department of Energy, under Award No. DE-NE0008653.

NOMENCLATURE

Gt	Gigatonne
UNF	Used Nuclear Fuel
FP	Fission Product
Ln	Lanthanide
MA	Minor Actinide
An	Actinide
MOX	Mixed Oxide Fuel
P&T	Partitioning and Transmutation
TRU	Transuranic
LLE	Liquid-Liquid Extraction
PUREX	Plutonium Uranium Redox EXtraction
UREX	Uranium Redox Extraction
TBP	Tributyl Phosphate
TRUEX	Transuranic Extraction
CMPO	Carbamoylmethylphosphine Oxide
DIAMEX	Diamide Extraction
DGA	Diglycolamide
NEXT	New Extraction System for TRU Recovery
TALSPEAK	Trivalent Actinide Lanthanide Separation by PhosphorousReagent Extraction

ORNL	Oak Ridge National Laboratory
DTPA	Diethyleneetriaminepentaacetic Acid
SLE	Solid-Liquid Extraction
UNH	Uranyl Nitrate Hexahydrate

TABLE OF CONTENTS

Page

LIST OF FIGURES

FIGURE Page

LIST OF TABLES

TABLE Page

1. INTRODUCTION

1.1 General Background

Currently, the world is facing difficulties concerning energy sources and how these sources will be employed in the future. Within this century Goodstein has assessed that oil resources will run out and the world will require an alternative energy source.[1] In fact, the depletion of oil could create chaos worldwide, as developing and established countries squabble over remaining energy resources.[1] It is also important to monitor the development of energy industries in developing countries, as there might be temptation to use harmful energy production techniques, for the environment or the general population, to achieve short term benefits. Currently the global population is about 7.5 billion and is projected to double within the next century.[1] The growth of world energy consumption is directly correlated to the growth in world population, meaning doubling in the world's population would likely cause exponential growth of the world's energy consumption. Furthermore, it is very likely that the continued increase of carbon emissions will have a direct impact on the degradation of the planet.[2] Thus it is it is essential to depend on non-carbon emitting energy sources that can provide the world with reliable and clean power, and one which can be expanded and modified to fit world needs. Nash et al., has stated that nuclear power may be the most rational approach to sustaining the world's energy needs and avoiding the increase of greenhouse gas in the atmosphere.[2]

The atmospheric carbon concentration was estimated to be 275 ppm in 1900, 370 ppm in 2000, and is projected to be 550 ppm in 2100. Currently the world consumes energy from an installed capacity of 18 TW of power, with 85% being contributed by fossil fuel energy. This data is from 2002 and, while likely reduced, the majority of our power is still produced through the use of fossil fuels. In order to stabilize the carbon concentration in the atmosphere at 550 ppm, the world would need to an installed capacity of 15 TW of power, free of carbon emission. Ewing[3] explains that:

Nuclear power provides approximately 7% of the world's electricity, which is equivalent to a reduction in carbon emissions of ~0.5 gigatons (Gt) of C/yr. This is a modest reduction as compared with global emissions of carbon, ~7 Gt C/yr. Most analyses suggest, that in order to have a significant and timely impact on carbon emissions, carbon-free sources, such as nuclear power, would have to expand total production of energy by factors of three to ten by 2050. A three-fold increase in nuclear power capacity would result in a projected reduction in carbon emissions of 1 to 2 Gt C/yr, depending on the type of carbon-based energy source that is displaced.

The reduction of carbon emissions is clearly a large obstacle but one that can be overcome. Nuclear fission energy is the only power industry that has the potential to be scaled to meet world energy needs. In 2002, an assessment and comparison of the performances of different contemporary energy sources was conducted.[4] The energy sources performances were judged based on the present state and future potential of the

sources for four different categories: greenhouse gas emissions, acid precipitation (SO_2 and NO_x emissions), land requirement, and energy payback ratio. Energy payback is defined as the amount of energy produced per energy required for building and maintenance. The energy types compared were hydropower, coal, nuclear, natural gas, fuel cells, biomass plantation, sawmill wastes, wind, and solar (photovoltaics) energy. Using these categories hydropower, nuclear, and wind energy rank highest as the most viable and environmentally-friendly sources. While solar energy has advanced rapidly in the last decade and, though it's land requirements can be reduced by placing solar cells on top of houses, it and wind energy are only intermittent sources that cannot produce energy around the clock. Hydropower is also a very good candidate for a renewable source of energy under these criteria, however it cannot easily be scaled to meet world energy needs due to land and water requirements. Nuclear energy does very well in the emissions category and has the smallest land requirements of any source. The nuclear energy payback ratio scores well considering the drawbacks of the other energy sources; however, this referenced report does not assess the issue with nuclear waste disposal and its safety. The strategy of partitioning and transmutation can be implemented to reduce the negative environmental effects of nuclear fuel storage.

Currently, in the U.S., used nuclear fuel (UNF) storage is a huge issue and is only getting larger. With no permanent repository, or even a clear repository implementation plan in place, about 70,000 metric tons of UNF sit in wet and dry cask storage, as of 2013.[5] This number is estimated to be the maximum capacity for the previously prepared

nuclear repository site, Yucca Mountain, and is expected to double within the next 30 years, if the generating capacity remains constant.[5] The Yucca Mountain UNF storage site implementation has been cancelled, due to social and political controversy. Due to the United States' Nuclear Waste Disposal Act created in 1982, the government is being sued for having no current primary or secondary waste disposal, as of 1998.[6] In 2008 another lawsuit was filed due to no geologic storage. Xcel Energy and other companies have agreed to settlements with the Department of Energy to receive a monetary refund for the government's inability to deal with UNF. "The Department of Energy projects that these payments will rise to $ 0.5 billion per year after 2020 if it does not take custody of the fuel."[7] If the nuclear energy industry is to be expanded to meet growing demand for emission-free energy, then a disposal plan must be made for the deferred UNF. While 99% of the UNF in a repository will decay within 300 years a significant portion of the fuel and fission products (FP) will remain for hundreds of thousands of years. These remaining elements still emit a large amount of radiation after the 300 years. Attempting to create a structure with a plan for it to last a few hundred thousand years into the future can be very problematic.[2] This is because there are a multitude of dissolution pathways for UNF that could occur while in geologic repository at Yucca Mountain, which could lead to contamination of groundwater among other issues.[8] Below in Figure 1, the decay rate of the different components of UNF and the fission products is shown.

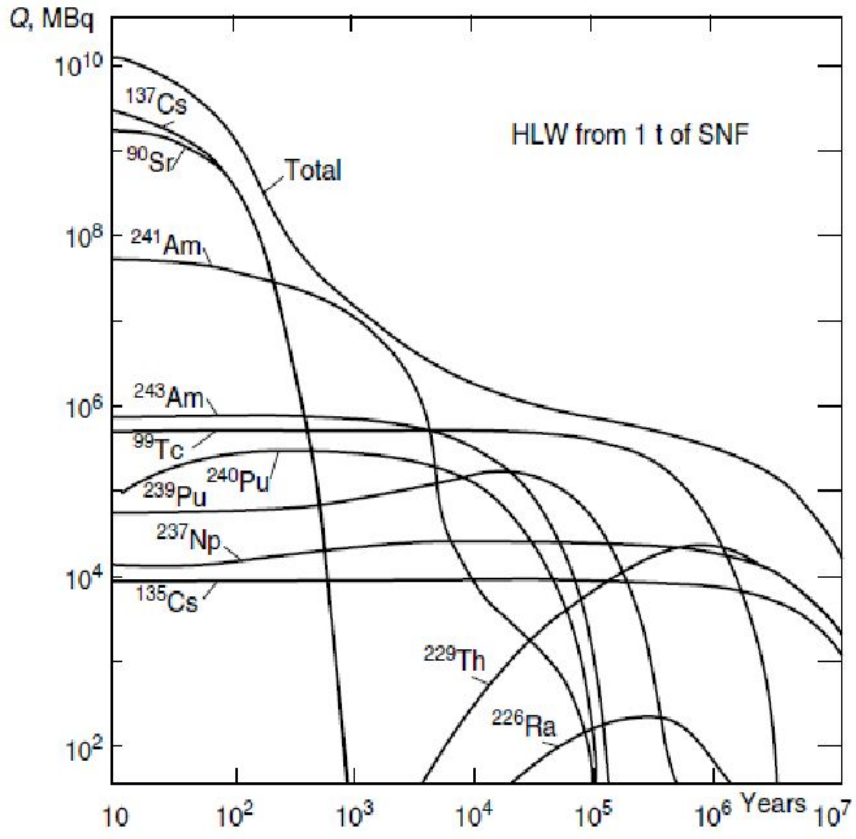

Figure 1: Activity distribution of 1 ton of high-level waste in megabecquerels over time. © 2012 Lázár K, Máthé Z. Published in[9] under CC BY 3.0 license. Available from: http://dx.doi.org/10.5772/48123. Reprinted

It can be seen that, in one ton of UNF, the transuranic elements last about 100,000 years and contribute a high level of activity to the total waste. As an example of how long this waste stays radioactive, Am-243 and Np-236 have half-lives of 7,370 and 154,000 years, respectively. 10 years after removal from a reactor the surface dose rate of a UNF assembly is about 10,000 rem/hr which is much higher than a fatal dose for humans (about 500 rem received at one time would cause serious illness and can be

potentially fatal).[10] Only about 4% of the uranium in nuclear fuel is used for power generation. The remaining 95% of the useable uranium is disposed with the other nuclear waste, due to a buildup of heavy elements which cause neutron poisoning. Lanthanide (Ln) fission products are generally most liable for neutron poisoning, specifically Sm, Gd, and Eu.[11] With no definite plan for a safe and permanent way to store this used fuel, it is clear a recycle process needs to be developed to reduce the large amount of fissionable material currently planned for disposal. Partitioning and transmutation of this UNF is a viable method for managing the waste disposal and potentially its re-use in the nuclear fuel cycle. The term "partitioning" refers to the removal of the U through Am nuclides from UNF. The term "transmutation" is the process of converting one isotope into another by means of nuclear reactions. In this case the objective is to convert the minor actinides (MAs) separated from the waste into either shorter-lived products or stable products through neutron interaction in a reactor.[12] In fact, even if disposal was not an issue for the nuclear waste, wasting 95% of the fuel should be seen as unacceptable for a finite resource. This problem needs to be addressed and can be done so by closing the nuclear fuel cycle by instituting partitioning and transmutation.

In the U.S., as of now, the nuclear fuel cycle is not actually a cycle at all. The open and closed nuclear fuel cycle can be seen in Figure 2.

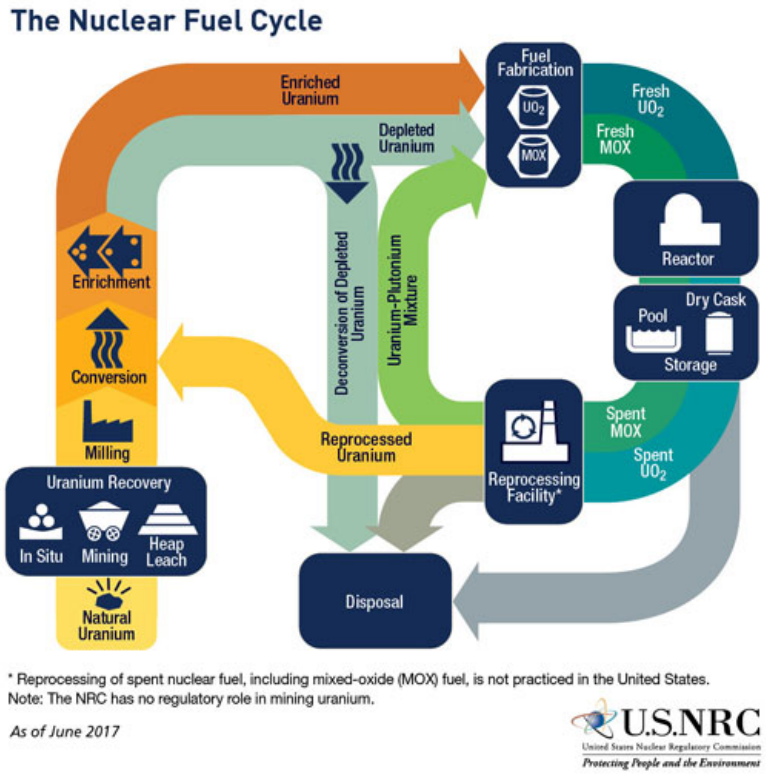

Figure 2: The different stages and paths of a closed nuclear fuel cycle published June, 2017. Reprinted with permission from[10]

The two cycles consist of the front end, middle, and back end. The front end is composed of mining, milling, enrichment and fuel fabrication. The middle of the fuel cycle is the burning of the fuel and collecting the energy produced from the fission. The back end is where the open and closed fuel cycles differ. In the current open nuclear fuel cycle, the fuel is simply sent to storage for disposal. It is in the closed nuclear fuel cycle, where partitioning can occur and allow the UNF to be recycled. The remaining material that cannot be recycled is then sent to disposal. Two fundamental ways the world utilizes the fuel cycle for an increase in energy production are through a closed fuel cycle and

combination of reactor types “such as, thermal and fast neutron reactors”.[3] Neutron energies have a significant effect on what fission products are produced in a reactor, and fast neutrons can best consume long-lived actinides (Ans) while fission is occurring. The amount and type of nuclear waste a fissile material produces in a reactor depends on the fuel type and burn time of the reactor. “As an example, a ^{232}Th-based fuel cycle can be used to breed fissile ^{233}U with minimum production of Pu”.[3] While breeder reactors are not utilized in the United States, this transmutation of the MAs through burnup would be highly advantageous for the management of UNF. Uranium and plutonium can be separated and repurposed as a mixed-oxide (MOX) fuel. In a report on the future of nuclear fuel partitioning and transmutation (P&T)[13], Dusan Calic states that “P&T can reduce the radiotoxic inventory of spent fuel by a factor of 100 to 1,000 and can achieve the reduction of time needed to reach the radioactivity level of the uranium ore from 100,000 to 5,000 years”. This means the transuranic elements (TRU) must be separated from the long-lived fission products present in UNF in order to perform a transmutation of the actinides. The most efficient and cost-effective separation process and UNF storage strategy is being pursued by nuclear-capable countries. This separation can be very difficult because the actinides and lanthanides have very similar chemical properties, due to their trivalent electron clouds, and similar atomic radii. These elements also have oxidation states of +1 to +4, though U through Am can achieve higher oxidation states of up to +6. The similar properties of these Ans and Lns, are what cause the difficulty in separations of U through Am from fission products (FPs), which are mostly lanthanides. Am must also be separated from Cm for a transmutation of Am to be

possible.[14] Waste is also being created at each separation step due to the use of organic solvents in the process. An efficient and cost-effective separation process for this high-level waste is currently being pursued world-wide.

1.2 Partitioning Methods

Many nations around the world are pursuing research in the effort of developing an efficient and cost-effective method for reprocessing the unused 95% of uranium remaining in nuclear fuel, as well as any plutonium (1%) that is available. Currently liquid-liquid extractions (LLE) dominate the field using aqueous and organic solvents. However, in these LLE methods, hydrolysis and radiolysis are large issues, causing the solvent to degrade and create third phases which can reduce the effectiveness of the separation. This is why it can be advantageous to use solid separations methods.[13] This section describes the various aqueous and non-aqueous methods that have been highly developed and their potential drawbacks.

Solvent extraction processes separate compounds or complexes into an organic or aqueous phase, using an extractant ligand.[2] This ligand is designed to chemically partition the desired element or elements from their starting solution with high selectivity and efficiency. This process is shown in Figure 3.

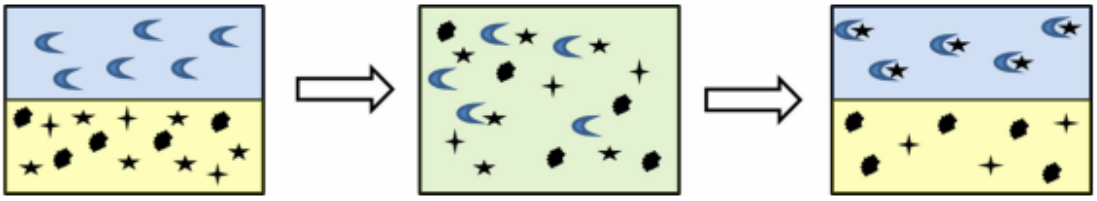

Figure 3: A general solvent extraction process. An organic phase (upper blue) containing an extracting agent (blue crescent), is mixed with an aqueous phase (lower yellow) containing a desired metal ion (black star) and undesired metal ions (remaining black figures). Reprinted from[17]

The ideal solvent would be hydrolytically and radiolytically stable, and easy to produce. There are a large number of solvent extraction processes that have been developed that are specialized for certain elements and have certain properties like a resistance to high radiation energy. Aqueous extraction methods, commonly employed in UNF reprocessing can be separated into three groups: the extraction of U and Pu from UNF, the extraction of both transuranics and Lns, and the partitioning of Ans from Lns. The first of these methods are the PUREX and UREX processes. The plutonium uranium redox extraction process (PUREX) is the only reprocessing method that has been widely used as an industrial scale process.[16] The report states that there are two methods by which the process can be performed. The first is the full PUREX process, and utilizes the ligand tributyl phosphate (TBP) (30% in kerosene) to extract Pu(IV) and U(VI) out of a UNF solution dissolved in 3–6 M nitric acid.[16,17] “Oxalic and hydrofluoric acids can be added to prevent unwanted extraction of molybdenum (Mo) and zirconium (Zr)”.[17] The aqueous phase is then separated from the solution leaving U and Pu in the organic phase. In PUREX a reducing agent, N,N-dihexyl octanamide, is added to the solution and Pu

and U can be re-introduced to nitric acid, for conversion to MOX, to be used as fuel in current reactors or fast reactors. In the second version of the process, named the uranium extraction process (UREX), the U and Pu are separated into an organic phase as before, however a reducing agent is added to the solution that is specific to Pu and causes the formation of Pu(III) which is then separated from the U. It is necessary to repeat this process multiple times to achieve a high separation factor for the desired elements. TBP is cheap, simple and selective for tetra- and hexavalent Ans, and is hydrolytically stable. However, TBP can be radiolytically degraded to form a new compound under radiation, which creates a third phase in a solution and hinders the separation process, producing a large amount of unnecessary excess waste, specifically phosphates. The PUREX process is one of the most studied and well understood separation processes but a drawback to this method is that it cannot extract Am from the UNF. PUREX also can no longer be used in the U.S.[17]

The processes that involve the co-extraction of transuranics and Lns are the TRUEX and DIAMEX processes. The transuranic extraction process (TRUEX) is a modified version of PUREX where the trivalent MAs and Np(V) are extracted with Pu(IV) and U(IV) by adding the extractant carbamoylmethylphosphine oxide (CMPO) in the organic phase.[17] The main reason this method was developed is to extract trivalent Am from UNF, since a large portion of alpha activity is caused by ^{241}Am.[18] Normally, chemical and radiolytic degradation of CMPO occurs, leading to radiolytic and hydrolytic waste products that occur in the PUREX process. Like TRUEX, the diamide

extraction process (DIAMEX), partitions the Ans and Lns from UNF. DIAMEX is an extraction process developed by France to handle UNF disposal in an easier manner without using hazardous organic solvents.[17] It uses a diglycolamide (DGA) as its solvent extractant, which has been seen to form complexes with Am(III) and Pu(IV).[17] These extractants can be incinerated, and when they are degraded they do not form harmful compounds but require high acid concentrations to perform separations and have a "greater tendency toward third phase formation".[16]

Finally, the CYANEX and TALSPEAK processes involve the separation of the Ans from the Lns. The CYANEX process involves a group of extractant compounds that originate from the organo-dithio-phosphinates family and Cyanex-301.[17] It has a very high separation factor between the Ans and Lns specifically one of about 40,000 for Am and Eu[19], however disposal of this solvent is difficult. A large change in the pH of the feed stream is required to perform this separation which is undesirable in a large process.[16] The trivalent actinide lanthanide separation by phosphorous reagent extraction (TALSPEAK) process was developed at Oak Ridge National Labs (ORNL). TALSPEAK uses the extractant di(2-ethylhexyl)phosphoric acid (D2EHPA) to extract Lns from the aqueous phase, which contains diethylenetriaminepentaacetic acid (DTPA). Lactic acid is part of the aqueous medium to improve phase transfer kinetics and act as a coextractant of the Lns while the Ans remain complexed with DTPA.[19] Lactic acid "scavenges" ·OH radicals, protecting the extractants from radiolytic degradation.[15] However it is still difficult to dispose these extractants as they inevitably contain free

radicals produced from radiolysis. The organic solvent benzene is also required for this extraction which further complicates the waste disposal for this process.

There are also a set of processes dedicated to the separation of Am and Cm, however these methods are not widely developed as this separation is one of the most difficult due to chemical and atomic similarities between these two elements.[20] The separation of Am and Cm is a very difficult process, but it is necessary for the transmutation of Am in a fast reactor after the reprocessing is completed. This is because transmutation is difficult for a single element, and the complexity of the plan for transmutation could drastically increase with each element added. Another reason this separation is desired is because it would allow isotopic analysis to be done on Am, which is currently difficult due to the physical and chemical similarities between these two elements.[21] There are multiple processes which have been developed previously to perform this separation, however it would be highly advantageous to perform it in a single step without the addition of any organic solvents, and in conjunction with separation of the Ans U, Pu, and Np.[14,22]

Using solid sorbents instead of liquid extraction solvents presents many advantages such as the avoidance of organic waste that is resultant from solvent degradation, no third phase formation, and faster kinetics. While these solid sorbents are organic-based, they are chosen for their hydrolytic, radiolytic, and chemical stability as well as high porosity, which is necessary to deal with large volumes of UNF solutions

and prevent degradation. Similar extractant ligands are generally used in these solid materials that will sorb the actinides from the UNF solution. The materials used are polymer resins, porous silica, polymer membranes, metal oxide particles, clays, carbon-based materials or magnetic nanoparticles.[17] Solid sorbents are advantageous to LLE methods at a lab scale, but the largest drawback to this technology is its lack of industry testing. According to Nash et al.[23], it is unclear how this new technology would hold up to repeated loading and radiolysis/hydroloysis. The solid sorbents produce similar waste products as their LLE counter parts, however the long residence times required for these processes' extractions could contribute to inefficiency of these techniques in the long term.

Pyrochemical processes are an example of another technology that could diligently perform transuranic separations which would create less waste required for disposal. To perform these separations UNF metal salts are placed in a cathode-basket and heated to over 800 °C. These metal salts are then reduced and transferred to the anode, and based on the potential, the actinides can be separated using the electro-refiner. The development of fast reactors may decide whether this becomes a viable process since it uses molten salt fuel which thus produces a metal UNF that can be pyrochemically processed.[24] Implementing this type of separation process requires large steps towards commercialization. This technology also is best suited to complement the use of advanced fast reactors, which have not been implemented due to political concerns related to nuclear proliferation. The high temperatures and corrosivity of the

molten salts required for this technology also make these materials difficult to handle in large scale processes.[19]

Though these processes have potential to aid in the partitioning and transmutation of UNF, each have significant issues. Generally multiple separation methods can be combined to remove U through Am from the remaining Ans and fission products, however many steps must be used to process this high-level waste in preparation for geologic storage. No implemented process exists to perform the separation of the U through Am from the MAs and Cm, efficiently in a single step, thus multiple separations are used to process high-level waste. Since separation factors are generally low for each of these processes, they must be repeated multiple times to achieve the desired separation factor. Each repetition introduces more organic solvents that require processing before disposal. With multiple processes being performed many times, a large amount of unnecessary waste is created. The process being augmented in this work and described in the next sub-section is a group actinide separation of the Ans, U through Am, and is a solid-liquid extraction (SLE), which uses no organic solvents and achieves what the previously described processes intend with a reduced amount of steps (potentially only one), with little to no waste added to the process. This process is the crystallization of U through Am, and effectively processes high-level waste in a single step.

1.3 Separation through Co-Crystallization

Batch crystallization is a widely used method throughout many industries generally for separations and purification processes. It was first attempted in Germany to purify uranium from the PUREX process.[25] More than 90% of the uranium was recovered as uranyl nitrate hexahydrate (UNH)[26] crystals shown below:

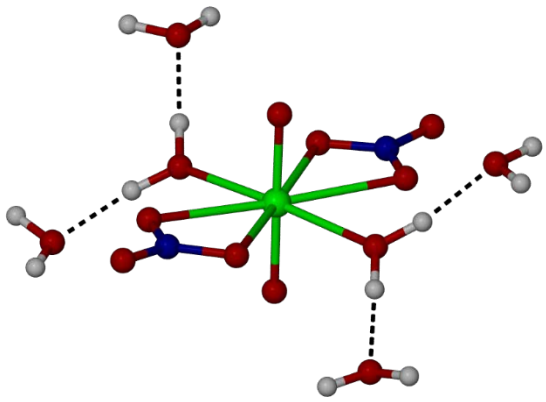

Figure 4: Molecular structure of the linear dioxocation UNH. Reprinted with permission from[26]. Copyright (2016) American Chemical Society.

The other transuranic elements and fission products remained in solution, when this crystallization was performed. This process also resulted in a high decontamination factor of about 100 for both Pu and Cs. This initial crystallization of UNH paved a way for this research, and a new type of separation technique. In the Japan Atomic Energy Agency, work has been under progress to create a disposal technique based around fast neutron reactor fuel, titled the New Extraction System for TRU Recovery (NEXT).[25]

This process involves the crystallization, using a simple reduction in temperature to reduce the solubility limit of U for its recovery, the co-recovery of U, Pu, and Np using TBP as an extractant, and the recovery of Am, and Cm using extraction chromatography. This crystallization technique has many advantages over other reprocessing methods as it only requires HNO_3 and a reduction in temperature to begin crystallization of uranium to UNH. The crystallization is designed to reduce the load on the extractant which removes U, Pu, and Np. This dissolution of the UNF in HNO_3 is already common practice in this industry and this acid is relatively easy to clean up.[25]

In a HNO_3 solution, U ions are crystallized as UNH by the following reaction:

$$UO_2^{2+} + 2NO_3^- + 6H_2O \leftrightarrow UO_2(NO_3)_2 \cdot 6H_2O \qquad (1)$$

As shown in the reaction above, uranium must be oxidized to crystallize into UNH. This crystal is a linear dioxocation that is only formed with the metals U, Pu, Np, and Am, and has not been observed for any other element on the periodic table. The precipitation of this distinct compound out of solution allows uranium to be easily separated from used nuclear fuel in a simple step. Crystal structures can become contaminated by impurities, originating from the mother liquor, which appear as inclusions in a crystal structure. In the NEXT process a washing step was studied to determine if these impurities could be removed.[27] Washing these crystals in nitric acid was found to increase the decontamination factor of Ce, however the U yield was decreased due to UNH's propensity towards dissolution in low HNO_3 concentrations. Subsequent washing steps resulted in diminishing returns.[28]

In another study, Nakahara et al.[29], determined how Pu and HNO_3 concentrations affected various solid fission product impurity behaviors such as $Cs_2Pu(NO_3)_6$ and $Ba(NO_3)_2$ crystallization. Eu was easily washed away with HNO_3 and the DF of Ba was very low, but neither was affected by Pu or HNO_3 concentrations. The DF of Cs tends to decrease with high concentrations of HNO_3 and Pu in the mother liquor, causing the precipitation of $Cs_2Pu(NO_3)_6$.[30].

The group crystallization of the hexavalent actinides, U through Am, can achieve, in a single step, what normally requires many separate aqueous processes and produces large volumes of waste.[26] In this study, Burns et al. initially confirmed that only hexavalent ions were being proportionally removed from solution with UNH, suggesting that a co-crystallization was indeed occurring. Next, a co-crystallization of the actinides U through Am was achieved in near proportion by oxidizing each to their hexavalent state using $NaBiO_3$. In their hexavalent state, the actinides form a chemically distinct compound that is not observed elsewhere in the periodic table, and it is likely that these hexavalent dioxocations of Am, Pu, and Np replace UO_2^{2+} in the crystal structure of UNH as crystallization takes place. An increase in recovery of U was observed when using a low initial acid concentration. This solution became increasingly more acidic as the co-crystallization occurred, due to the reduction in volume of the solution and no acid being crystallized with uranium. This is advantageous because U solubility is high in low acidity HNO_3, so a large amount of UNH can be dissolved in a starting low acidity system, and, as the system is cooled, a higher ending acidity relates to a lower

solubility limit of U, pushing the crystallization process creating a greater crystal yield. A slow cooling was also found to increase the selectivity of the process from common fission products. However when the co-crystallization of U through Am was performed with a the addition of a spike of FPs present, the FPs were removed, albeit to a lesser extent, with U(VI). This experiment was performed in a highly oxidizing environment created by the presence of $NaBiO_3$ in solution. It is possible that some interaction between the FPs and this oxidizing environment is what caused the reduction in this decontamination factor. Regardless of this interaction, the separation of Am is one of the most important components of this process, since it is so essential in reducing the long-term radiotoxicity of UNF. Methods for this oxidation and separation process are currently being investigated by multiple research groups.

1.4 Oxidation of Americium

The oxidation of Am, specifically to its hexavalent state, is a very challenging problem, as the high redox couple of Am(III)/Am(VI) of ~1.68 V, in acidic media, makes this oxidation difficult to produce.[21,26] A very strong oxidizing agent is required to perform this reaction and this highly oxidizing system could potentially inhibit the separation and yield of UNH. AmO^{2+} is also a very unstable ion and will quickly reduce to Am^{3+} when a suitable oxidizing agent is not present or in the presence of organic compounds.[22] Sodium bismuthate is a very strong oxidizing agent, as the Bi(V)/Bi(III) redox couple is 2.0 V, making this compound an appealing option for this work. Ammonium peroxydisulfate can also be used as an oxidizing agent for Am(III)/Am(VI),

however this agent decomposes in low nitric acid concentrations to form hydrogen peroxide which can reduce Am(VI). This is not favorable due to the widespread use of HNO_3 currently in reprocessing processes, and likely would not be a good oxidizing agent for a separation of Am from UNF. Sodium bismuthate, however, has been observed to oxidize Am^{3+} to its hexavalent state in highly acidic solutions, which is very favorable as these are the types of solutions that the UNF will be dissolved in.[14,31] In the co-crystallization of the actinides U through Am it was discovered that when Am(VI) was incorporated into the crystalline phase, stability in this hexavalent state greatly increased, with no reduction in Am(VI) after 13 days, when $NaBiO_3$ was employed as an oxidizing agent for this separation. The introduction of $NaBiO_3$ was also found to enhance separation of U for the process.[26] Sodium bismuthate is also easily procured and relatively cheap. With these advantages in mind, it seems pragmatic to choose bismuthate as an oxidizing agent for large scale processes involving the oxidation of the actinides, U through Am. However sodium bismuthate is not highly soluble in nitric acid and its slow dissolution kinetics could prove to be a problem for a quick oxidation of Am to its hexavalent state.[31] Sodium bismuthate has also not been well studied and little is known about its inorganic oxidation properties, as well as its interactions with heavy metal ions. Research must be done to better understand how the dissolution behavior of sodium bismuthate is affected by a complex system, like that of a UNF feed stream.

1.5 Objectives

This thesis will focus on studying the kinetic and thermodynamic properties of the dissolution of sodium bismuthate by nitric acid and the effects of other metal ions in solution on these properties. Specifically, this study is interested in determining the dissolution rate and solubility limit for sodium bismuthate in nitric acid systems. The effect of secondary ions on the dissolution behavior of sodium bismuthate in nitric acid will also be investigated, with particular interest on metals present in used nuclear fuel, like U, and key fission products. The metal ions Cs^{+}, Sr^{2+}, Nd^{3+}, Zr^{4+}, and Ce^{3+} will be introduced to these systems as fission product surrogates as a representation of the various fission products and oxidation states common in UNF. Chapter 2 describes the materials, experimental setup, and experiments performed for this research, Chapter 3 details the results and provides a discussion of their interpretation. Chapter 4 presents the conclusions of the study and the possible future directions and applications of the techniques discussed.

2. MATERIALS AND METHODS

2.1 Introduction

As stated previously, sodium bismuthate works as a viable oxidizing agent for Am(III)/Am(VI), it also has a long shelf life, and is widely commercially available. To employ sodium bismuthate as an oxidizing agent in the nuclear fuel cycle however, its thermodynamic and kinetic properties must first be understood in conditions which mimic a UNF feed stream. This chapter is designed to provide an account of the materials used and procedures that were necessary to provide a clear and complete understanding of subsequent chapters. This chapter is divided into five parts. The first is the introductory section. The second is the various materials required throughout this research. The third section describes the process used to characterize sodium bismuthate particles. Finally, in the fourth section the experimental methods for determining the solubility limit and dissolution rate of sodium bismuthate in varying systems is discussed.

2.2 Materials

Nitric acid (69–70% Omni Trace, HNO_3) was purchased from EDM; cerium(III) nitrate hexahydrate (99.5%, $Ce(NO_3)_3 \cdot 6H_2O$), cesium nitrate (99.8%, $CsNO_3$), neodymium(III) nitrate hydrate (99.99%, $Nd(NO_3)_3 \cdot nH_2O$), sodium bismuthate (ACS Grade, $NaBiO_3$), strontium nitrate (99.0%, $Sr(NO_3)_2$), and zirconyl chloride octahydrate (98%, $ZrOCl_2 \cdot 8H_2O$) were all purchased from Alfa Aesar; depleted uranyl nitrate hexahydrate (ACS Grade ≥80%, $UO_2(NO_3)_2 \cdot 6H_2O$) was purchased from SPI Supplies and all were used as received. Deionized (DI) H_2O was obtained from an ELGA LabWater Purelab Flex ultrapure laboratory water purification system operated at 18.2 MΩ cm at 25 °C.

2.3 Sodium Bismuthate Powder Characterization

Scanning electron microscopy (SEM) was performed to determine the particle size distribution using a JEOL 6400 Scanning Electron Microscope housed in the Fuel Cycle and Materials Laboratory at Texas A&M University. The SEM electron beam was operated at 15 keV, and the images recorded the back-scattered electron (BSE) detector signal. All samples were carbon coated prior to imaging. ImageJ software was then used to determine the size distribution and average size of the particles. This analysis software was calibrated to the magnification of each image, the image was altered to increase the contrast between the particles and the background, this image was duplicated, and filtered with a Gaussian blurr and processed in order to subtract any background

interference from the original image. The particle sizes were then determined by simply measuring the distance across each particle. It was assumed that particles with an area greater than ~80 μm^2 were an agglomeration of multiple particles and were not counted in the analysis.

The density of the $NaBiO_3$ powder was determined by submersing approximately 1,552.8 mg of powder in 5,000 µL of DI H_2O and measuring the displacement of the H_2O. The powder was thoroughly mixed with the solution and allowed to settle before the displacement was measured to ensure complete wetting of the sample.

2.4 Solubility and Dissolution Kinetics of Sodium Bismuthate

Small batch experiments were performed by mixing 1,000 µL solutions of varying nitric acid concentrations of roughly 4.3–6.0 M HNO_3, containing Sr, Zr, Cs, Ce, Nd, or U at a concentration ranging from 50–250 mM with 500 mg of $NaBiO_3$ powder, shown below in Tables 1-7. Aliquots were sampled periodically, diluted, and analyzed by inductively-coupled plasma mass spectrometry (ICP-MS) with a Perkin Elmer NexION 300D ICP-MS to determine the concentration of metals in solutions. Before sampling each solution was centrifuged at RPM for 5-10 min in a SCILOGEX D1008 mini-centrifuge, to ensure undissolved bismuthate was not present in the aliquot to be analyzed. After sampling, the experiments were agitated to ensure thorough mixing of solid with the solution.

Table 1: Total amounts of sodium bismuthate, nitric acid, and DI H_2O used to perform a control dissolution experiment of bismuthate in only Nitric acid.

Experiment	$NaBiO_3$ (mg)	HNO_3 (µL)	H_2O (µL)
4.3 M HNO3 Control	500.0	272	728
5.0 M HNO3 Control	498.5	316	684
6.0 M HNO3 Control	496.6	380	620

Table 2: Material amounts and conditions used to perform a dissolution experiment of bismuthate with cerium present.

Experiment	$NaBiO_3$ (mg)	Conc. HNO_3 (µL)	H_2O (µL)	Ce Stock (507 mM [Ce]) (µL)
50 mM [Ce] 4.3 M [HNO_3]	505.6	266	635	99
150 mM [Ce] 4.3 M [HNO_3]	495.8	253	451	296
250 mM [Ce] 4.3 M [HNO_3]	498.0	241	266	493
50 mM [Ce] 5 M [HNO_3]	500.5	310	591	99
50 mM [Ce] 6 M [HNO_3]	495.6	373	528	99

Table 3: Material amounts and conditions used to perform a dissolution experiment of bismuthate with cesium.

Experiment	$NaBiO_3$ (mg)	Conc. HNO_3 (µL)	H_2O (µL)	Cs Stock (µL) (565 mM [Cs])
50 mM [Cs] 4.3 M [HNO3]	505.4	267	645	88
150 mM [Cs] 4.3 M [HNO3]	503.6	255	479	266
250 mM [Cs] 4.3 M [HNO3]	508.3	244	313	444
50 mM [Cs] 5 M [HNO3]	499.6	311	601	88
50 mM [Cs] 6 M [HNO3]	500.1	374	538	88

Table 4: Material amounts and conditions used to perform a dissolution experiment of bismuthate with neodymium present.

Experiment	$NaBiO_3$ (mg)	Conc. HNO_3 (µL)	H_2O (µL)	Nd Stock (µL) (823 mM [Nd])
50 mM [Nd] 4.3 M [HNO3]	504.3	268	671	61
150 mM [Nd] 4.3 M [HNO3]	501.4	261	557	182
250 mM [Nd] 4.3 M [HNO3]	505.8	253	443	304
50 mM [Nd] 5 M [HNO3]	499.8	313	626	61
50 mM [Nd] 6 M [HNO3]	500.9	376	563	61

Table 5: Material amounts and conditions used to perform a dissolution experiment of bismuthate with strontium present.

Experiment	$NaBiO_3$ (mg)	Conc. HNO_3 (µL)	H_2O (µL)	Sr Stock (µL) (1 M [Sr])
50 mM [Sr] 4.3 M [HNO3]	501.2	269	681	50
150 mM [Sr] 4.3 M [HNO3]	497.1	263	587	150
250 mM [Sr] 4.3 M [HNO3]	501.1	256	494	250
50 mM [Sr] 5 M [HNO3]	502.8	313	637	50
50 mM [Sr] 6 M [HNO3]	500.9	377	573	50

Table 6: Material amounts and conditions used to perform a dissolution experiment of bismuthate with uranium present.

Experiment	$NaBiO_3$ (mg)	Conc. HNO_3 (µL)	H_2O (µL)	U Stock (µL) (2.176 M [U])
50 mM [U] 4.3 M [HNO3]	504.3	272	705	23
150 mM [U] 4.3 M [HNO3]	511.1	272	659	69
250 mM [U] 4.3 M [HNO3]	504.9	272	613	115

Table 7: Material amounts and conditions used to perform a dissolution experiment of bismuthate with zirconium present.

Experiment	$NaBiO_3$ (mg)	Conc. HNO_3 (μL)	H_2O (μL)	Zr Stock (μL) (925 M [Zr])
50 mM [Sr] 4.3 M [HNO3]	499.6	269	677	54
150 mM [Sr] 4.3 M [HNO3]	498.7	262	576	162
250 mM [Sr] 4.3 M [HNO3]	503.2	255	475	270
50 mM [Sr] 5 M [HNO3]	502.2	313	633	54
50 mM [Sr] 6 M [HNO3]	507.3	376	570	54

3. RESULTS AND DISCUSSION

3.1 Reductive Dissolution Reactions

It is important to gain a fundamental understanding of the kinetic and thermodynamic properties that dictate the dissolution of $NaBiO_3$ in nitric acid systems. The dissolution reaction of $NaBiO_3$ in solution is:

$$NaBiO_{3_{(s)}} \rightarrow Na^{+}_{(aq)} + BiO^{-}_{3_{(aq)}} \qquad (2)$$

Due to the limited solubility of $NaBiO_3$ and its slow dissolution kinetics in nitric acid, it is believed that this reaction is the rate limiting step during oxidation. [8] $NaBiO_3$ is the only sodium salt that is insoluble in water and only slightly soluble in nitric acid. Once dissolved, bismuthate can oxidize a metal as follows:

$$6H^{+} + BiO_3{}^{-} + 2Ce^{3+} \rightarrow Bi^{3+} + 2Ce^{4+} + 3H_2O \qquad (3)$$

This reaction is important to note since Ce^{3+}/Ce^{4+} has a similar redox couple as Am(III)/Am(VI) of 1.72 V and 1.68 V, respectively. There will also likely be Ce^{3+} present in UNF. Equation 4 shows a possible reaction pathway for the oxidation of Am^{3+}.

$$10H^{+} + 3BiO_3^{-} + 2Am^{3+} \rightarrow 3Bi^{3+} + 2AmO_2^{2+} + 5H_2O \qquad (4)$$

Understanding how this reaction might occur under conditions analogous to that of a UNF feed stream is the goal of this research.

3.2 Inverse Cube Rate Law

In order to describe the dissolution of sodium bismuthate, particles were assumed to be monodispersed, spherical, and homogenous. It was also assumed that the rate of dissolution was proportional to the total surface area of the particle at a specific time. A rate expression can then be defined as:

$$\frac{dm}{dt} \alpha\, V[Bi]_t A_{sp,t} = m_0 A_{sp,0}(m_t/m_0)^{2/3} \quad (5)$$

where V is the volume of the system, m_0 and m_t are the masses of bismuth at time t=0 and time t, respectively, $[Bi]_t$ is the concentration of bismuth at time t, $A_{sp,0}$ and $A_{sp,t}$ are the specific surface areas of bismuth at time t=0 and time t, respectively. A simple inverse-cubic rate law can then be derived to describe this dissolution as:

$$1 - \left(\frac{m_t}{m_o}\right)^{\frac{1}{3}} = kt/\rho r_0 \quad (6)$$

where k is the rate constant, t is the time, r_0 is the initial radius of the bismuthate particles, and ρ is the density of sodium bismuthate. Since this analysis follows the dissolution of bismuthate through its changing concentration over time, the equation can be better expressed as:

$$\left(1 - \frac{[Bi]_t}{[Bi]_{Eq}}\right)^{1/3} = 1 - kt/\rho r_0 \quad (7)$$

where $[Bi]_t$ and $[Bi]_{Eq}$ are the concentrations of bismuth in solution at time t and the equilibrium point of the experiment, respectively.

3.3 Size and Density Determination of Sodium Bismuthate Particles

It is necessary to determine the average radius of the sodium bismuthate particles and to estimate its density, in order to calculate rate of dissolution, *k* (see Equation 7). The average radius of these particles was calculated by collecting SEM images of sodium bismuthate powder, and determining their size with ImageJ, a simple automatic image measurement application. Figures 5 and 6 show the SEM images of the particles at different magnifications. For this analysis, it was assumed that the particles were spherical, and that these particles retained their shape throughout this dissolution.

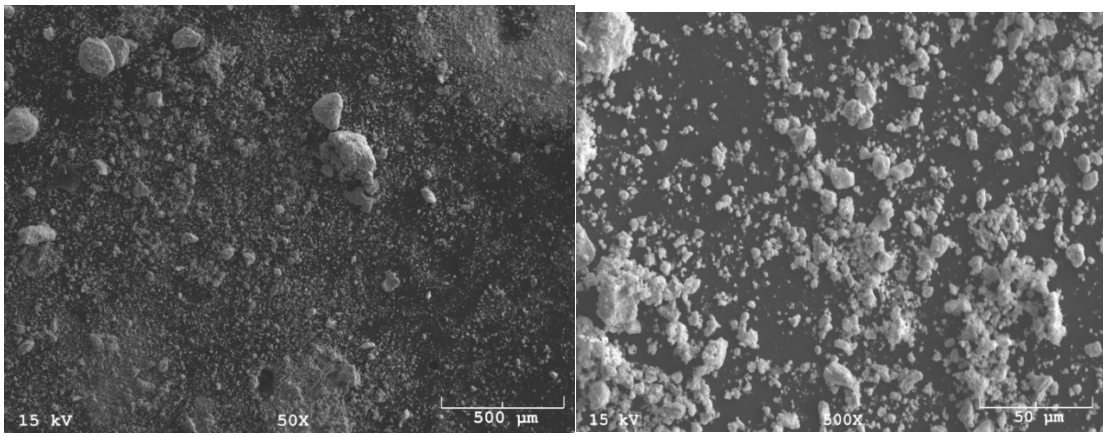

Figure 5: SEM image of sodium bismuthate at a magnification of 50x (left) and 500x (right).

As shown in Figure 6, the image contrast was increased and inverted to display the particles in black and the background in white. This image was then duplicated and filtered with a Gaussian Blurr. The blurred image was then subtracted from the original image to remove any uneven brightness on the particles that might interfere with measurements, to accurately judge the size of the particle. Shown below is the product of these efforts, and the final image used for particle size analysis. This same analysis was performed on multiple SEM images, which were taken at different areas of the sodium bismuthate sample to get an accurate average size estimate.

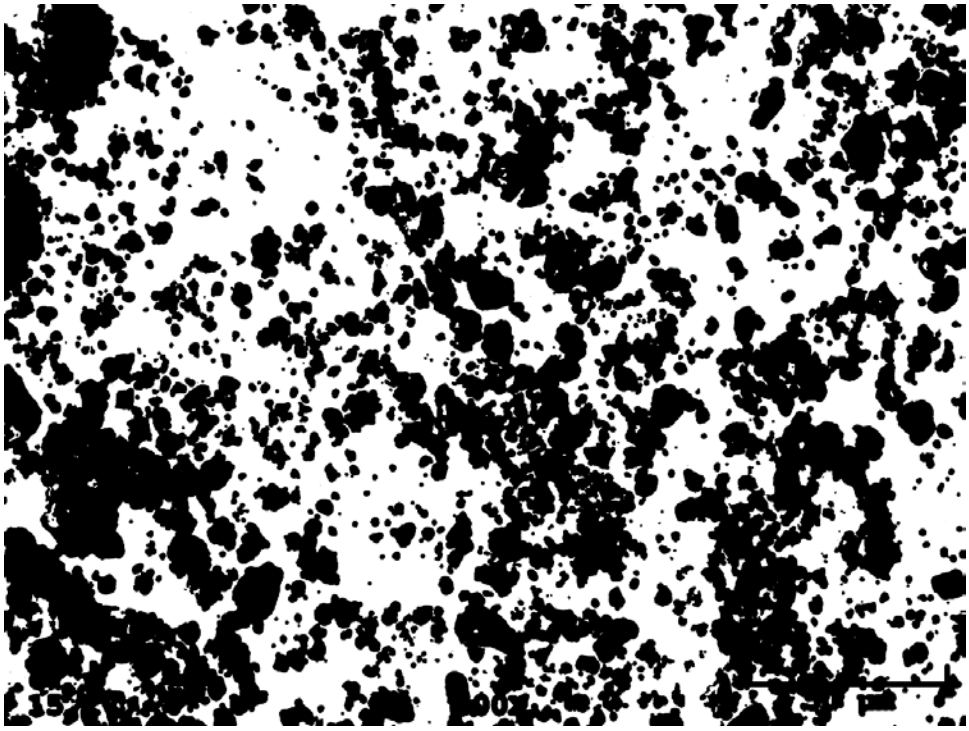

Figure 6: Modified high contrast SEM image.

The distribution of these particles is plotted below (see Figure 7). It can be argued that the larger particle sizes have a significant effect on the on the overall surface area of sodium bismuthate, and though the majority of particles fall within a small range of sizes, a mode cannot be used to determine average size, and these higher data points cannot be removed from analysis. It was determined that this set of data did not fit any distribution type, as it was compared in a probability plot to a normal, log-normal, and Weibull distribution. It can be seen in Figure 8 that the data clearly does not fit a Weibull or normal distribution. The logarithm of the data was taken and was found to not be in a normal distribution (see Figure 9), meaning the raw data does not fit a log-normal distribution. Thus the average particle size was calculated using the arithmetic mean of the data and was found to be 1.5 ± 1.0 μm. This large standard deviation is due to the large range of radii which can be ascribed to the process responsible for producing the powder, which is likely some form of grinding or milling. The minimum and maximum radii used for a cutoff point with these particles was 0.5 μm and 5.1 μm respectively. This was done intentionally, to prevent the measurement of multiple particles which were clumped together, which would disperse in solution, and to prevent measurement of any background specks in these images.

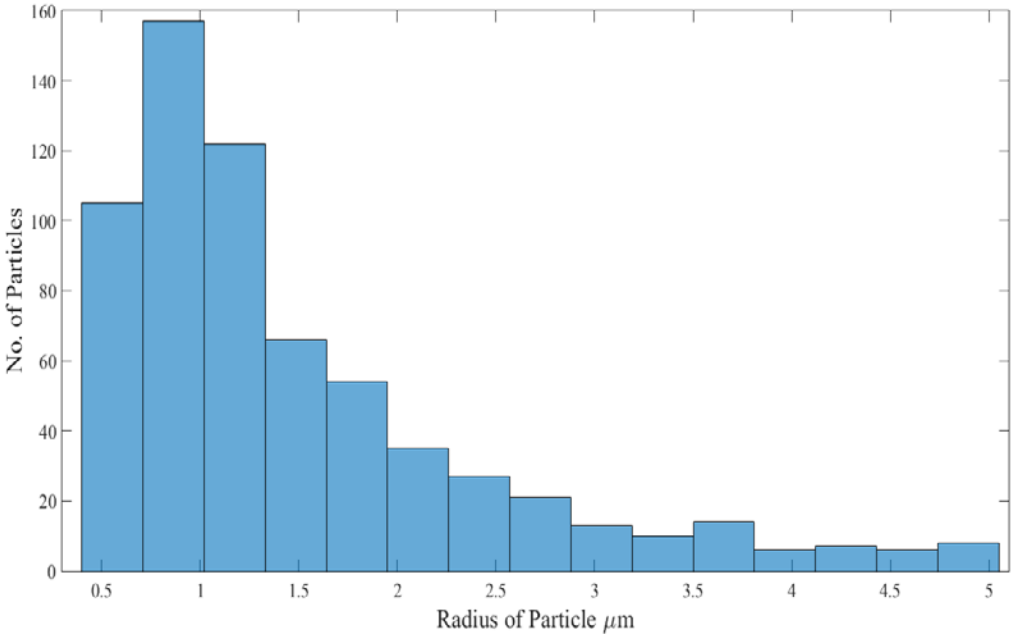

Figure 7: Histogram of the size distribution of sodium bismuthate particles.

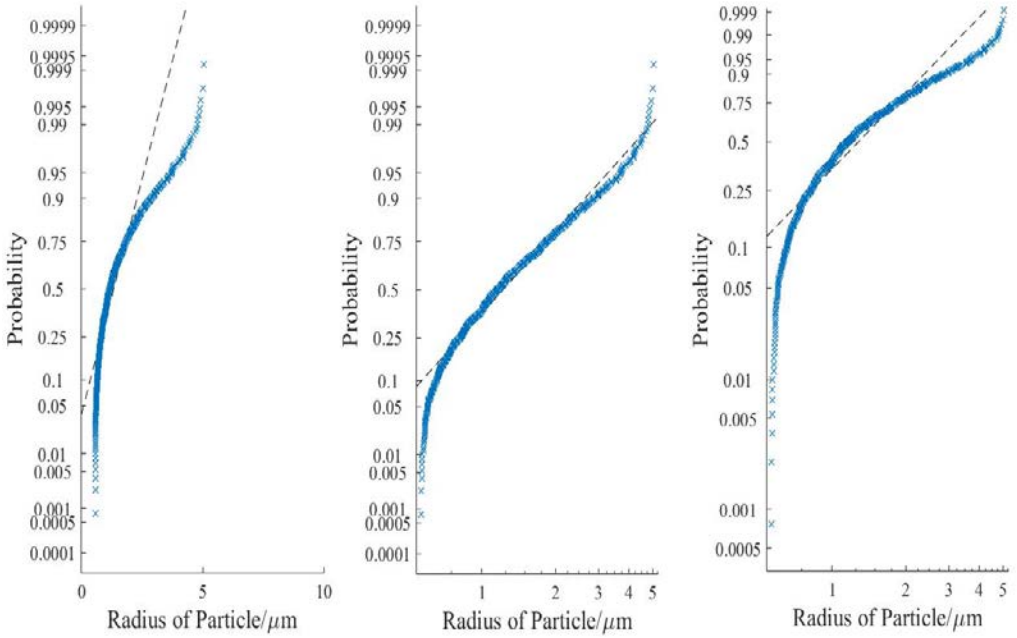

Figure 8: Probability plot comparisons of raw data against a normal distribution (left), log-normal distribution (middle), and Weibull distribution (right).

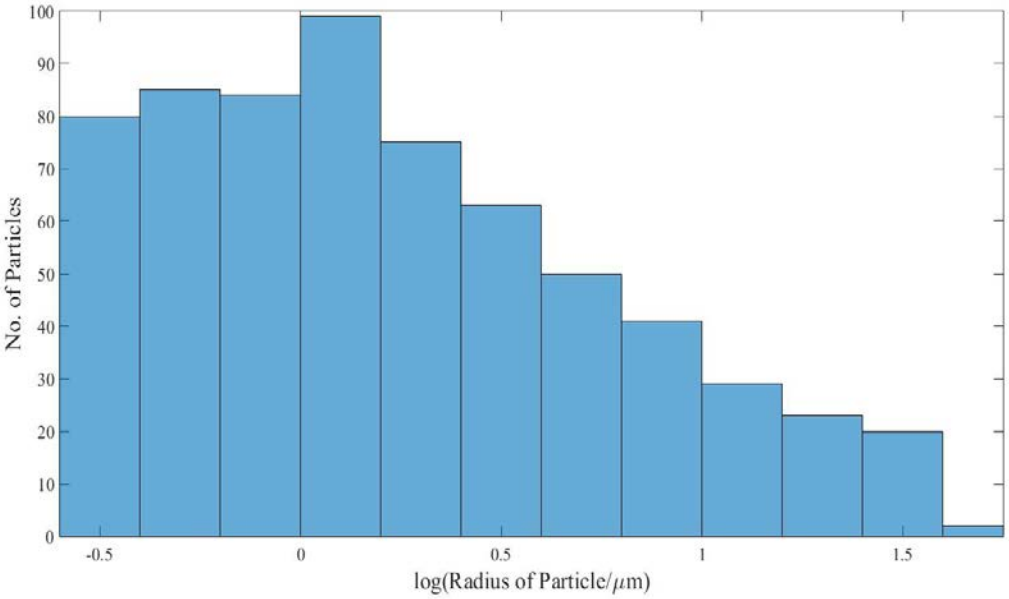

Figure 9: Histogram of the logarithm of size distribution of sodium bismuthate particles.

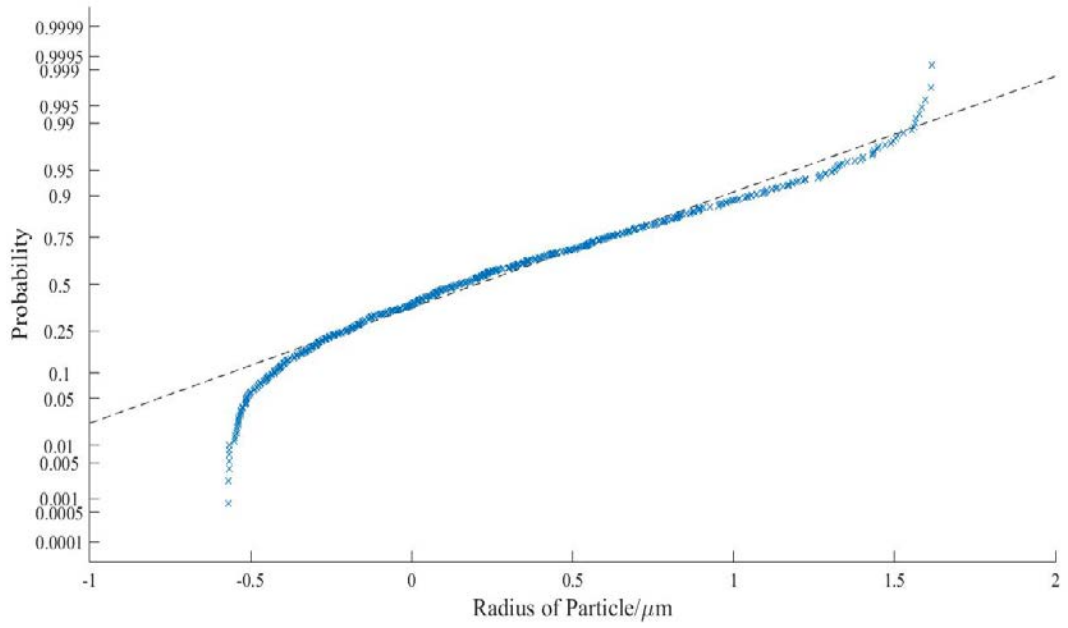

Figure 10: Probability plot of the logarithm of raw data against a normal distribution.

To determine the density of sodium bismuthate, a crude experiment was designed based on the equation:

$$\rho = \frac{m}{V} \qquad (8)$$

where, in this case, ρ is density of sodium bismuthate, m is the mass of the powder and V is the volume of the powder. This simple experiment described in Section 2.3 in Chapter 2 was performed, by adding 1552.8 mg of sodium bismuthate powder to 5000 μL of DI H_2O and measuring the displacement of the water. The change in volume was measured to be approximately 0.40 mL. Using these measurements, the density of sodium

bismuthate was calculated to be 3.9 g/cm^3. This value was consistent with literature values using similarly crude methods.[32]

3.4 Dissolution Properties of Sodium Bismuthate in Nitric Acid with Secondary Ions Present

First the dissolution rate and solubility limit of sodium bismuthate in nitric acid was examined. This was done to establish a baseline for an evaluation of how adding other metal ions to the system would change the rate of dissolution and solubility of sodium bismuthate. The acidity was varied between 4.3–6.0 M HNO_3 and was sampled over a period of 10 days. Figure 11 shows the results of these studies. It can be seen that the observed dissolution data does in fact follow the inverse cube rate law, shown in Equation 7. This shows that this equation was a good fit to describe this dissolution process and also implies that the rate of dissolution, *k*, found, is accurate.

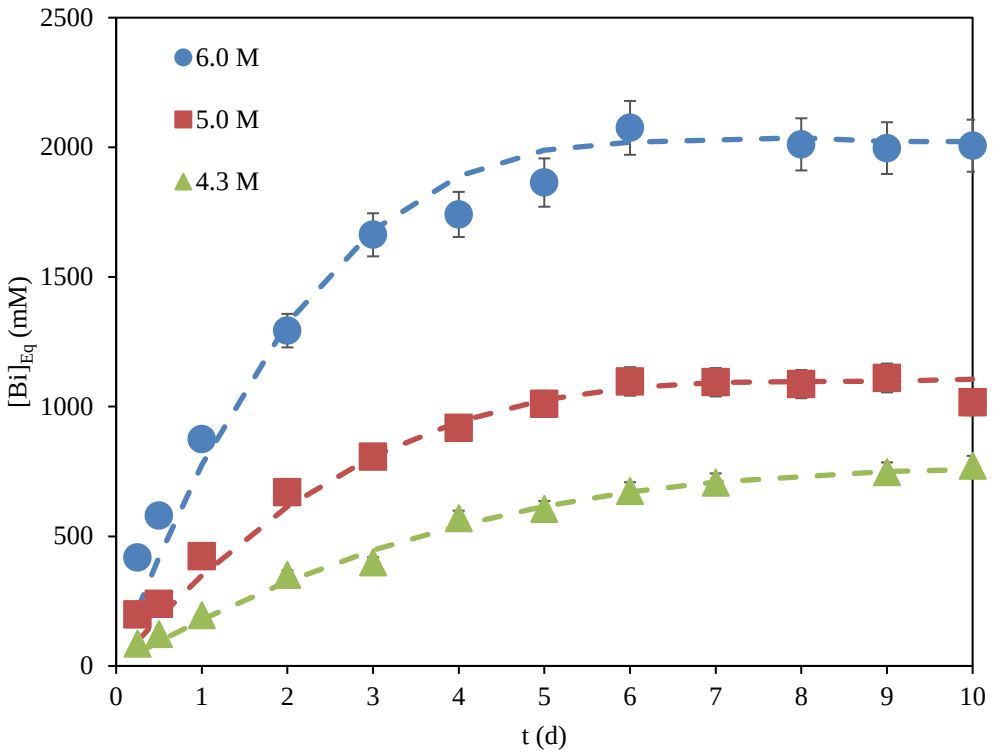

Figure 11: Dissolution of sodium bismuthate in 4.3, 5.0, and 6.0 M HNO_3 over ten days.

The rate and solubility of sodium bismuthate were calculated and plotted as a function of nitric acid concentration, as show in Table 8 and Figure 12. It can be seen that both the rate of dissolution and solubility limit of bismuth increase linearly, in this region, as a function of acidity. This is to be expected, as increasing the nitric acid concentration increases helps drive the dissolution of the sodium bismuthate, and helps stabilize the bismuthate ion. This preliminary experiment suggests that a system with a higher [HNO_3] would be more advantageous to dissolving a larger amount of sodium

bismuthate, rather than a system with a lower acidity. This is beneficial because UNF feed streams would likely be quite acidic, since HNO_3 is used to dissolve used fuel rods.

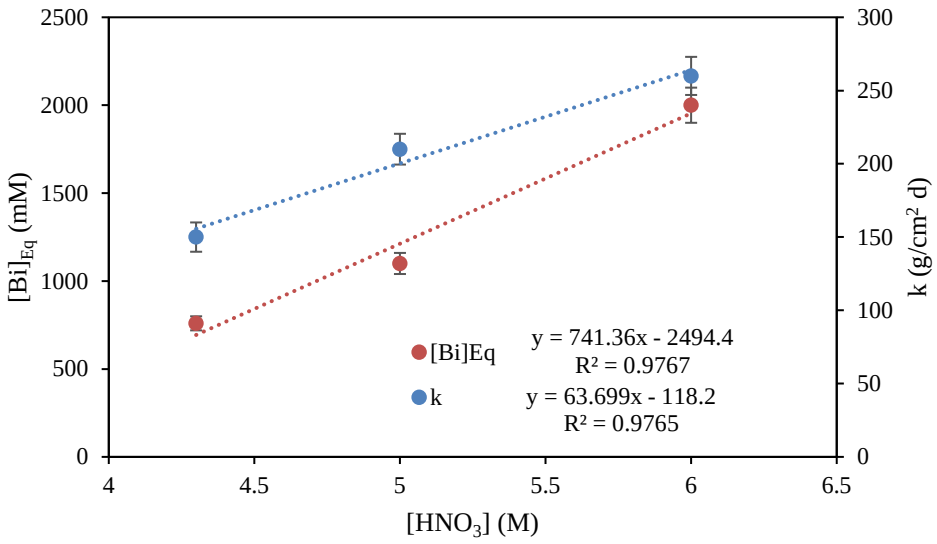

Figure 12: Correlation of solubility limit and dissolution rate vs. nitric acid concentration.

Table 8: Calculated dissolution rate and solubility limit values in nitric acid in the absence of surrogate materials.

$[HNO_3]$ (M)	k (g/cm^2 d)	$[Bi]_{Eq}$ (mM)
4.3	150 ± 10	760 ± 40
5.0	210 ± 10	1100 ± 60
6.0	260 ± 10	2000 ± 100

The following results describe how the dissolution rate and solubility limit of sodium bismuthate in nitric acid are affected by the presence of the FP's surrogates Cs^+, Sr^{2+}, Nd^{3+}, Zr^{4+}, and Ce^{3+} which will oxidize to Ce^{4+}. These surrogate FP's were chosen to represent the different oxidation states that are present in UNF feed streams. Ce and Nd were also chosen to represent the lanthanide series.

The effects of having Cs^+, a monovalent ion commonly found in UNF, present in solution was studied by first observing the solubility and rate of dissolution of sodium bismuthate as function of increasing Cs^+ concentration, while holding the nitric acid concentration constant at 4.3 M HNO_3 (see Figure 13). The dissolution rate and solubility limit of sodium bismuthate were calculated for the different Cs^+ concentrations and are displayed in Table 9. It can be seen from Figure 14 that the rate is only slightly impacted, if at all, by increasing the Cs^+ concentration. However, the solubility limit of

bismuthate is shown to have an indirect relationship with Cs^+ concentration, decreasing as the Cs^+ concentration increases. At this point it is not clear what the exact mechanism for this decrease in solubility is, but one explanation could be that Cs^+ is replacing Na^+ in the solid bismuthate phase, further reducing the solubility of the bismuthate solid phase. This would not be surprising, as it is a well-known trend, that as you go down Group 1, stronger binding is observed with larger anions. This is supported in Shriver and Atkins which describes enthalpies for the dissolution of a compound into its ions by the equations:

$$\Delta H_L \, \alpha \, \frac{1}{r_+ + r_-} \qquad (9)$$

$$\Delta_{hyd} H \, \alpha \frac{1}{r_+} + \frac{1}{r_-} \qquad (10)$$

where ΔH_L is the lattice enthalpy, $\Delta_{hyd} H$ is the enthalpy of hydration, r_+ is the radius of the cation, and r_- is the radius of the anion. These equations show that "size asymmetry can result in exothermic dissolution".

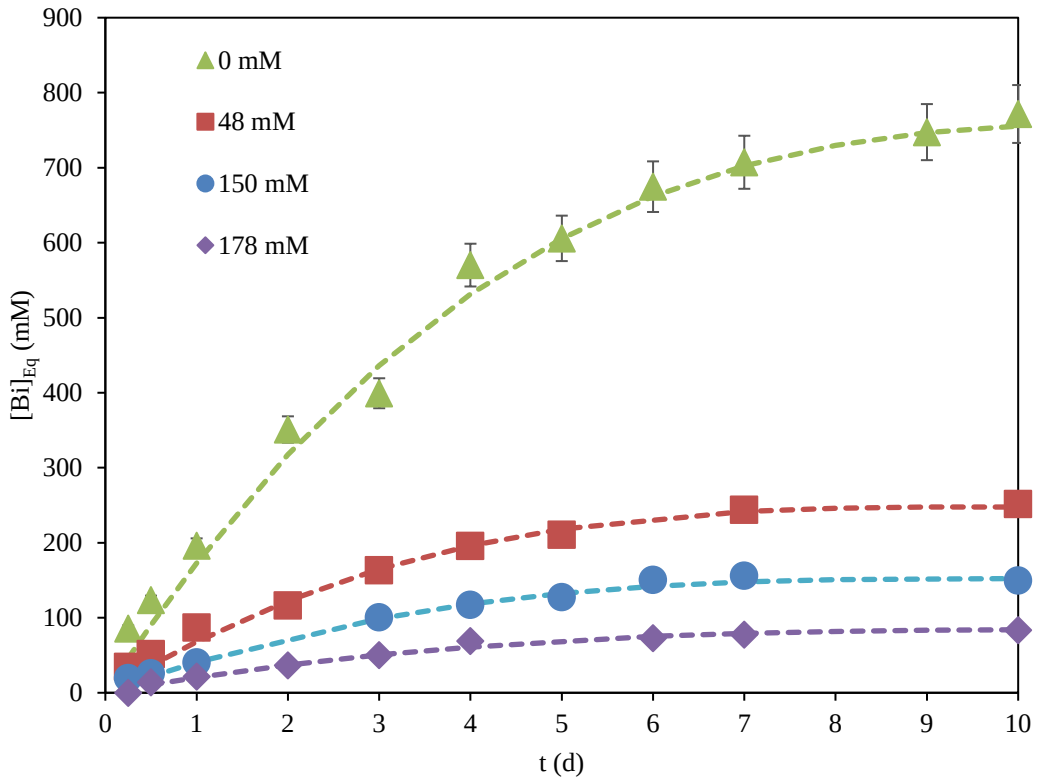

Figure 13: Dissolution of sodium bismuthate in 4.3M HNO_3 over ten days, with Cs^+ present.

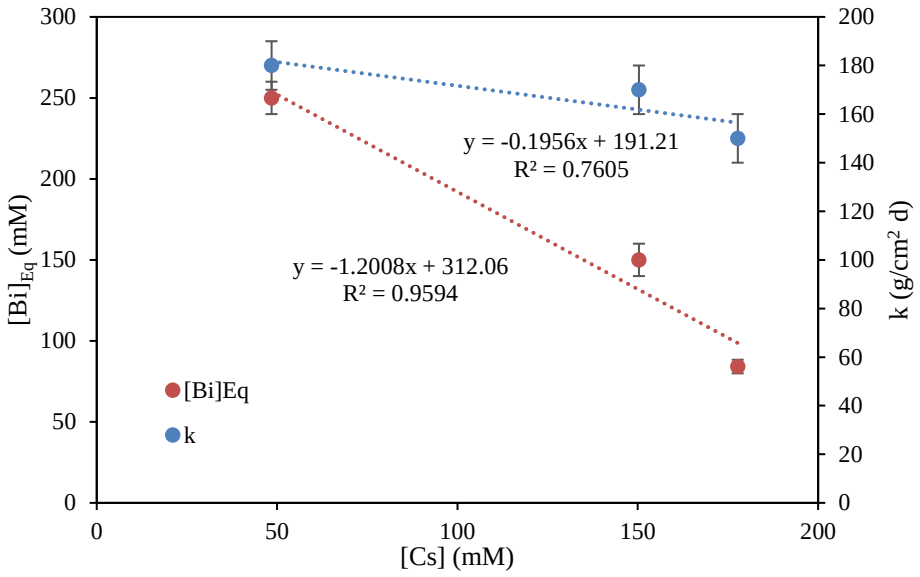

Figure 14: Solubility limit and dissolution rate of sodium bismuthate as a function of Cs^+ concentration.

Table 9: Calculated dissolution rate and solubility limit in 4.3 M HNO_3 as a function of Cs^+ concentration.

[Cs] (mM)	k (g/cm^2 d)	$[Bi]_{Eq}$ (mM)
0	150 ± 10	760 ± 40
48	180 ± 10	250 ± 10
150	170 ± 10	150 ± 10
180	150 ± 10	84 ± 4

The Cs^+ concentration was then held constant at roughly 50 mM and the nitric acid concentration was varied from 4.3–6.0 M (see Figure 15). As before, in the nitric

acid only system, both the solubility and dissolution rate of sodium bismuthate increase with an increase of acid concentration (see Table 10 and Figure 16). Upon increasing the nitric acid concentration to 5.0 M the dissolution rates were within error with those observed without Cs^+ present, where at 4.3 M HNO_3, the rate was slightly increased. The solubility of the bismuthate solid phase was reduced at all three acid concentrations compared to the nitric acid only system. However, the solubility limit was notably improved in higher acidity experiments. These results indicate that the presence of Cs^+ in solution has a negative impact on the dissolution of sodium bismuthate, which could hinder the oxidation process of actinides to their hexavalent stated in a recycle process.

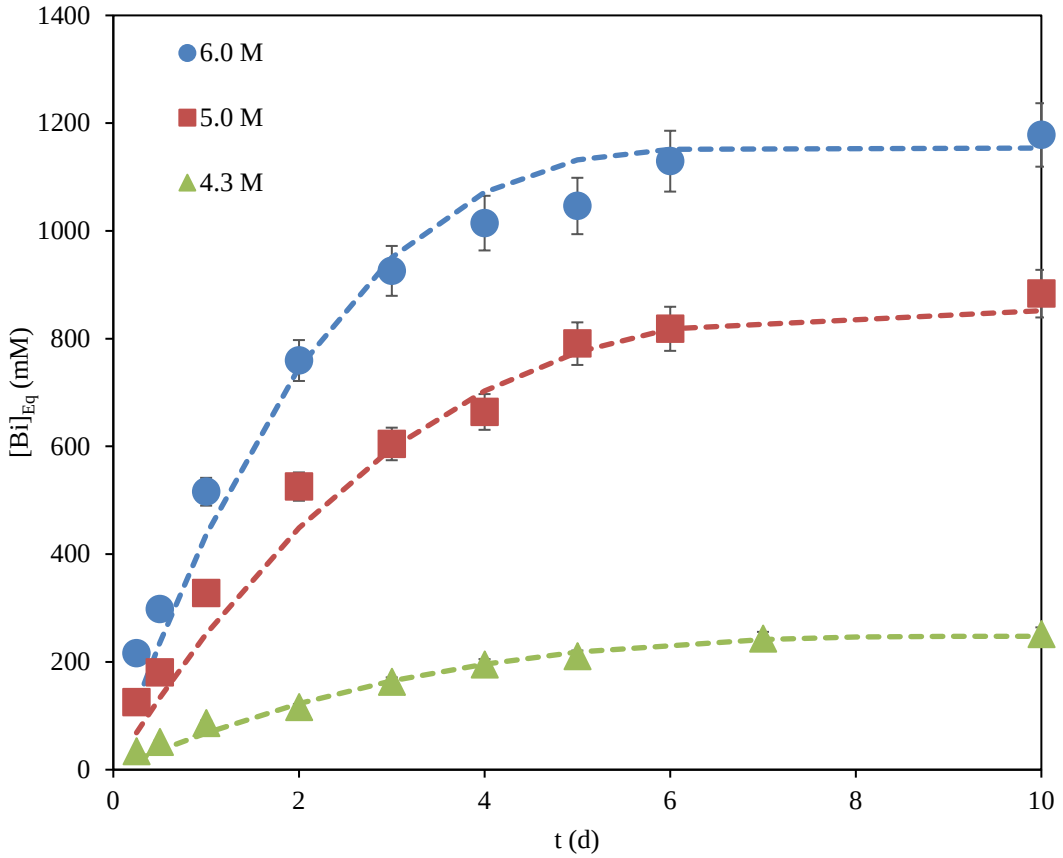

Figure 15: Dissolution of sodium bismuthate in 4.3, 5.0, and 6.0 M HNO_3 over ten days, with 50mM Cs^+ present.

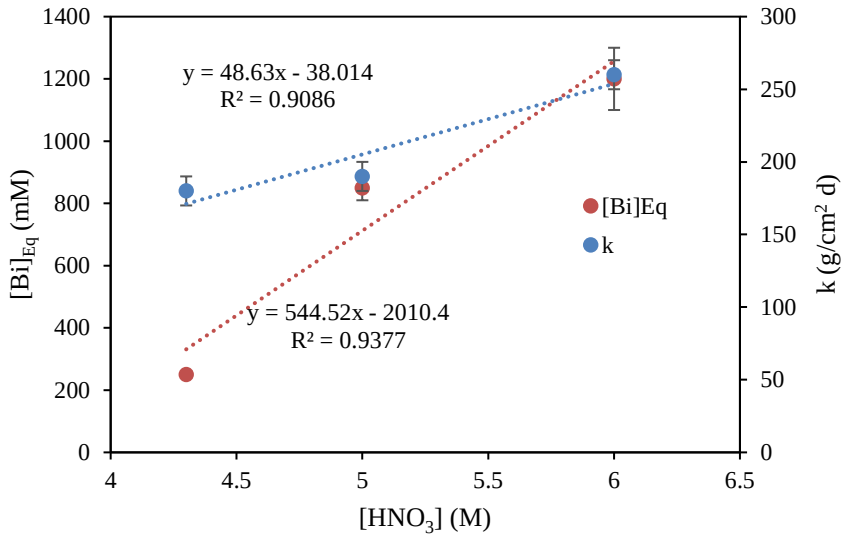

Figure 16: Solubility limit and dissolution rate as a function of acidity, with Cs^+ present.

Table 10: Calculated dissolution rate and solubility limit in the presence of roughly 50 mM Cs^+ as a function of HNO_3 concentration.

$[HNO_3]$ (M)	k (g/cm^2 d)	$[Bi]_{Eq}$ (mM)
4.3	180 ± 10	250 ± 10
5.0	190 ± 10	850 ± 40
6.0	260 ± 10	1200 ± 100

Next, it was of interest to gain an understanding of how a divalent metal would impact the system. Similar experiments were performed with Sr^{2+} as were conducted with Cs^+. In the case where the nitric acid concentration was held constant at 4.3 M and

the Sr^{2+} concentration was varied (see Figure 17), it can be seen in Table 11 that there is an increase in the rate of dissolution of about 40% between the Sr^{2+} and the nitric acid only system when Sr^{2+} is present at ~70 mM. This increase diminishes when the Sr^{2+} concentration is increased further. The solubility is relatively unaffected until concentration of Sr^{2+} reaches approximately 260 mM, where the equilibrium concentration of bismuth is reduced by about 25%. This reduction in solubility is most likely caused by the strontium ion behaving similarly to Bi^{3+} in solution, which is produced when bismuthate is reduced in the presence of water. This similar ion behavior reduces the amount of Bi^{3+} which can be produced, reducing the overall solubility limit of bismuthate.

In the case where the Sr^{2+} was held constant at approximately 50 mM, and the nitric acid concentration was varied, there was no observable change to that of the acid only system. The general conclusion that can be made from these experiment is that Sr^{2+} has almost no effect on the kinetic and thermodynamic properties of sodium bismuthate dissolution. There appears to be almost no interaction between Sr^{2+} and BiO_3^-, and that Sr^{2+} required very little solvent for dissolution, leaving the system mostly unperturbed.

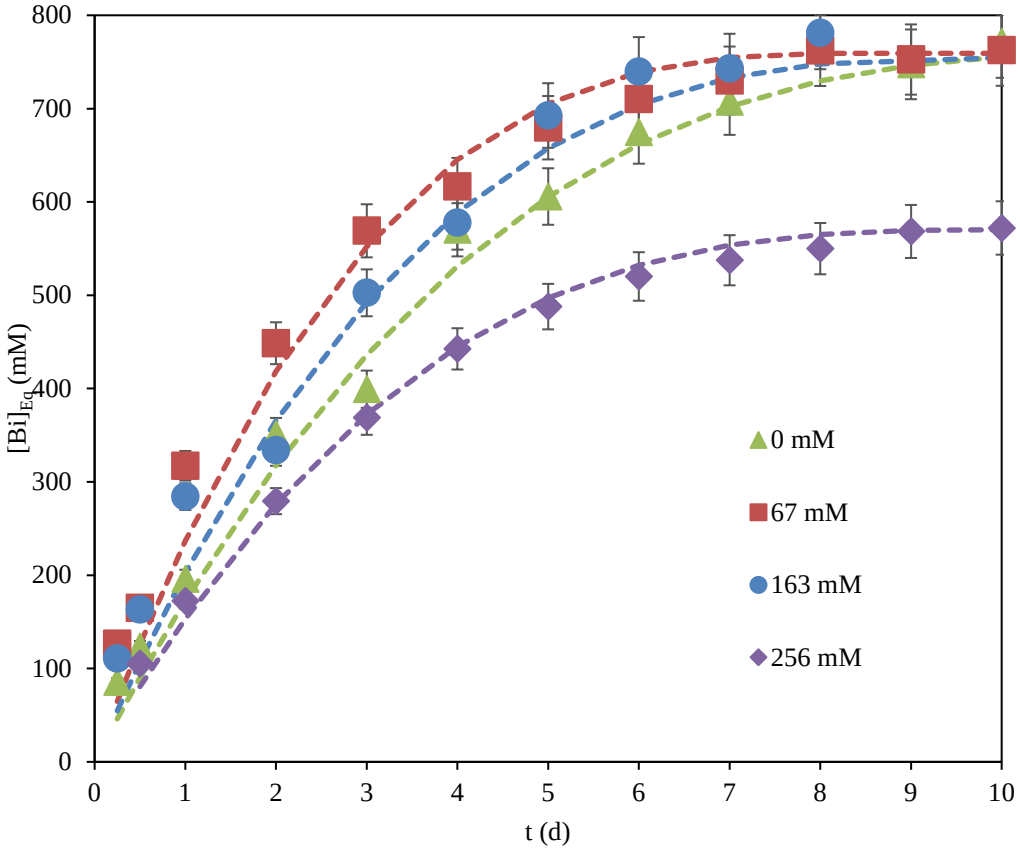

Figure 17: Dissolution of sodium bismuthate in 4.3M HNO_3 over ten days, with Sr^{2+} present.

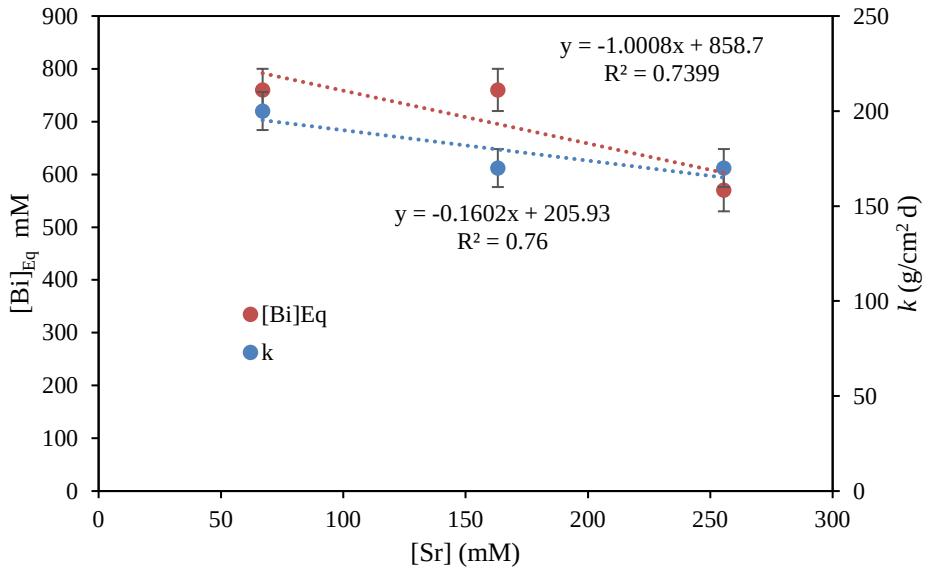

Figure 18: Solubility limit and dissolution rate of sodium bismuthate as a function of Sr^{2+} concentration.

Table 11: Calculated dissolution rate and solubility limit in 4.3 M HNO_3 as a function of Sr^{2+} concentration.

[Sr] (mM)	k (g/cm^2 d)	$[Bi]_{Eq}$ (mM)
0	150 ± 10	760 ± 40
67	200 ± 10	760 ± 40
160	170 ± 10	760 ± 40
260	170 ± 10	570 ± 30

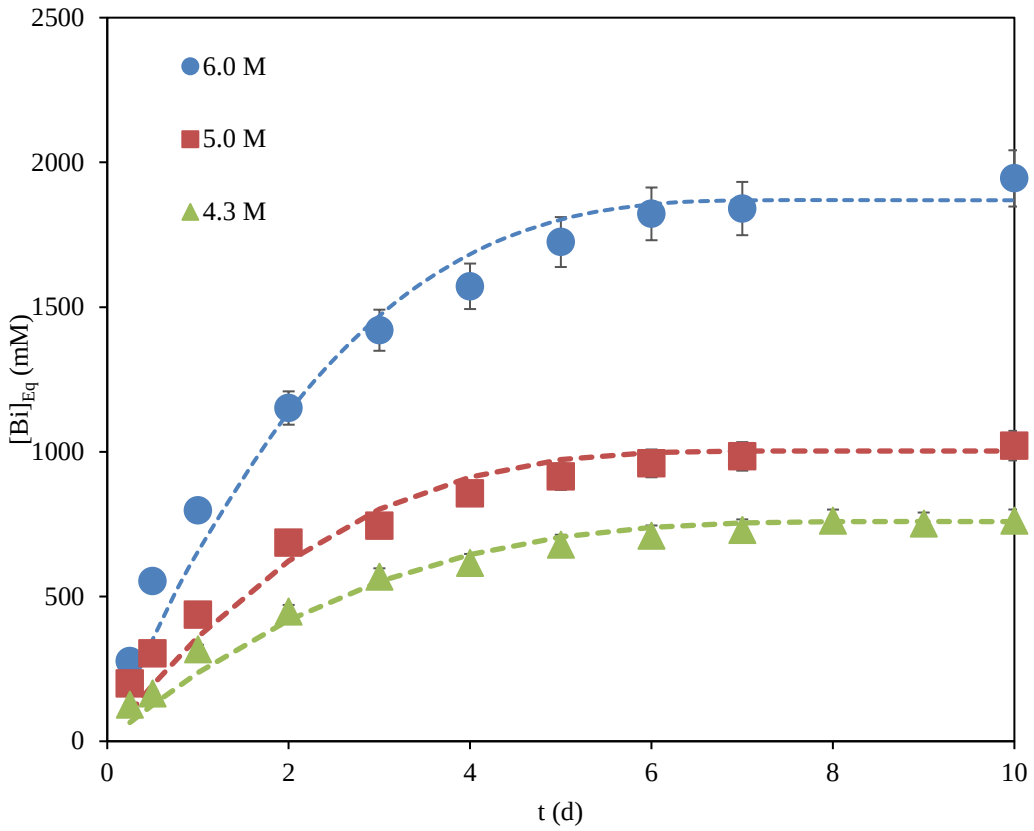

Figure 19: Dissolution of sodium bismuthate in 4.3, 5.0, and 6.0 M HNO_3 over ten days, with Sr^{2+} present.

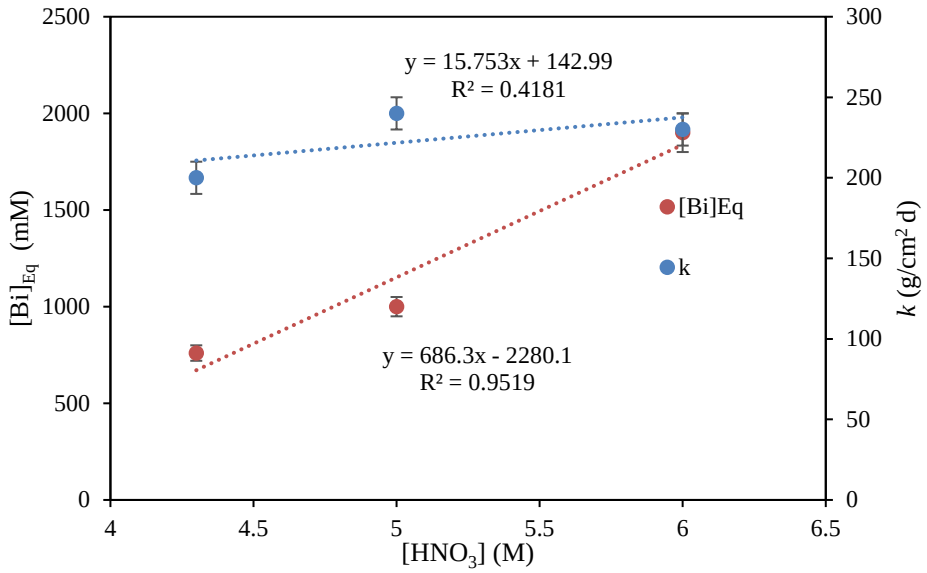

Figure 20: Solubility limit and dissolution rate as a function of acidity, with Sr^{2+} present.

Table 12: Calculated dissolution rate and solubility limit in the presence of roughly 50 mM Sr^{2+} as a function of HNO_3 concentration.

$[HNO_3]$ (M)	k (g/cm^2 d)	$[Bi]_{Eq}$ (mM)
4.3	200 ± 10	760 ± 40
5.0	240 ± 10	1000 ± 50
6.0	230 ± 10	1900 ± 100

The next set of experiments were performed to determine how the presence of Nd^{3+} would affect the dissolution behavior of sodium bismuthate. These experiments were performed similarly to those discussed above. It can be seen in Figure 21 that the

solubility limit of bismuthate decreased with an increase in neodymium, as the nitric acid concentration was held constant. When approximately 240 mM [Nd^{3+}] was present in solution a 25% decrease in the sodium bismuthate solubility limit was observed, compared to that in the acid only system (see Table 13). This indirect relationship can be attributed to the presence of Nd^{3+} in solution which likely created a common ion effect, where both Bi^{3+} and Nd^{3+} have the same charge and similar ionic radii, *ca.* 115 pm. The presence of Nd^{3+} appeared to have little effect on the rate of dissolution (see Table 12), and only marginally higher than the value found in the acid-only system.

In the experiments where the Nd^{3+} concentration was held constant at 79 mM [Nd^{3+}], a linear correlation was observed between the solubility limit of bismuthate, shown in Figure 24, with increasing the nitric acid concentration, in this range. In the case of the 4.3 and 5.0 M [HNO_3] experiments, a 15% decrease in sodium bismuthate's solubility was observed from the control experiments, however a 40% decrease in solubility was observed between the Nd^{3+} system and acid-only system when the acid concentration was further increased to 6.0 M [HNO_3]. This may be caused by a reaction between Bi^{3+} and NO_3^- to from an insoluble complex; however, no attempt to study this was made. The rate of dissolutions was mostly unchanged from the simple acid-only system, with the exception of 5.0 M [HNO_3], where a drop in rate was observed. The cause of this deviation is unclear at this time. From these studies, Nd might slightly hinder the oxidation of the actinides, U through Am, using bismuthate, but seemed to

have little effect on $NaBiO_3$ kinetics of dissolution and likely would not be a serious issue in a large-scale process.

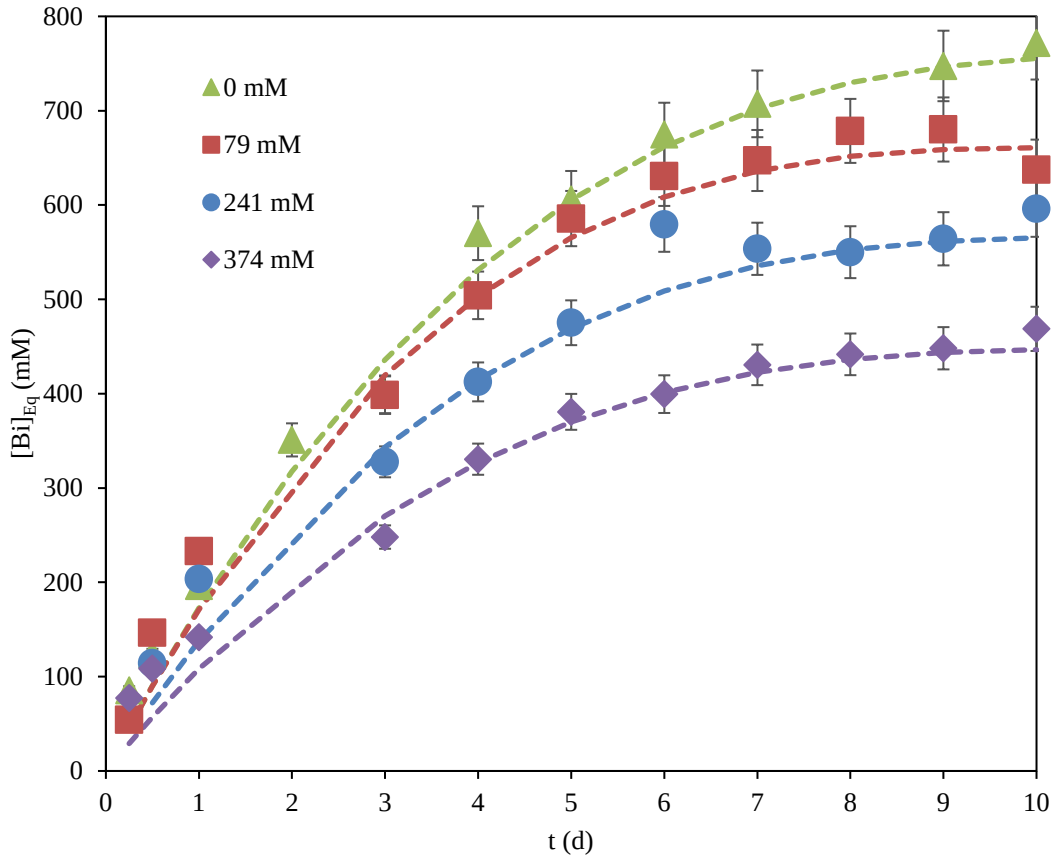

Figure 21: Dissolution of sodium bismuthate in 4.3M HNO_3 over ten days, with Nd^{3+} present.

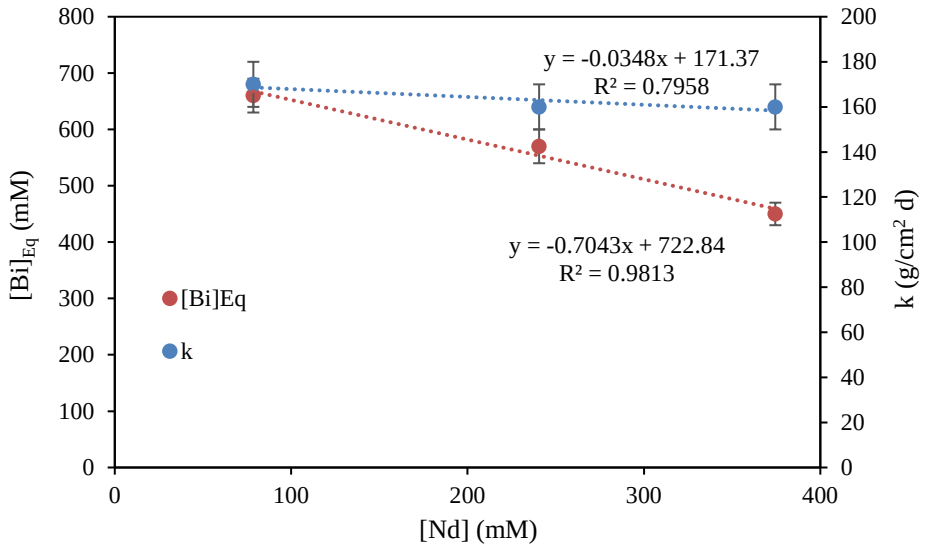

Figure 22: Solubility limit and dissolution rate of sodium bismuthate as a function of Nd^{3+} concentration.

Table 13: Calculated dissolution rate and solubility limit in 4.3 M HNO_3 as a function of Nd^{3+} concentration.

[Nd] (mM)	k (g/cm^2 d)	[Bi]$_{Eq}$ (mM)
0	150 ± 10	760 ± 40
79	170 ± 10	660 ± 30
240	160 ± 10	570 ± 30
370	160 ± 10	450 ± 20

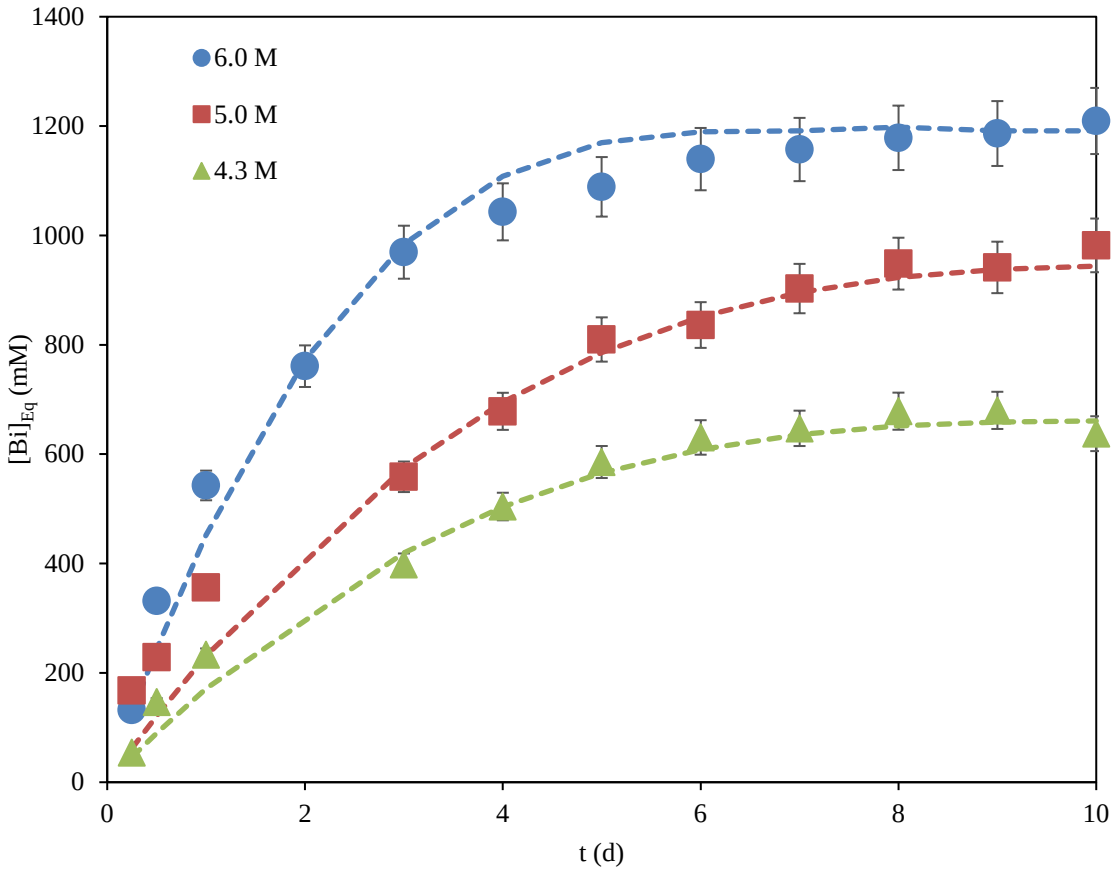

Figure 23: Dissolution of sodium bismuthate in 4.3, 5.0, and 6.0 M HNO_3 over ten days, with Nd^{3+} present.

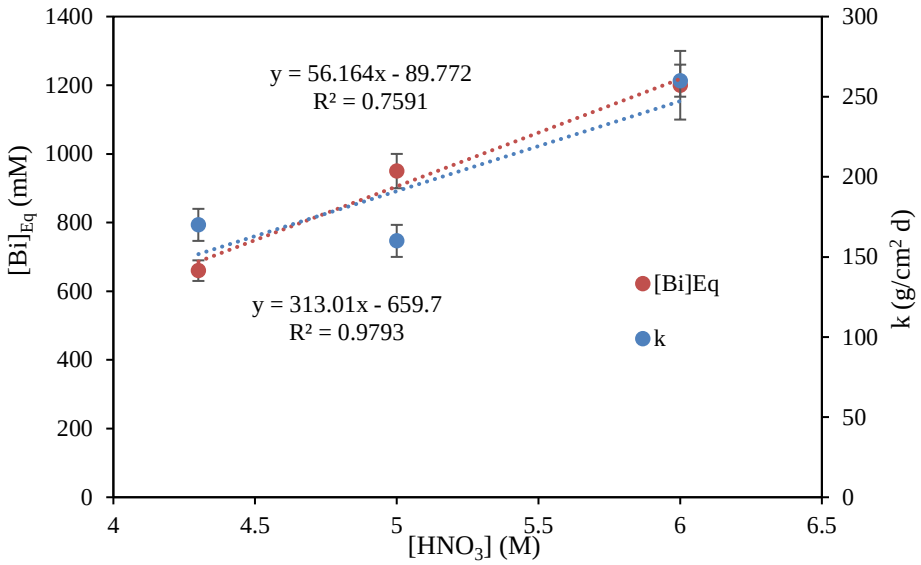

Figure 24: Solubility limit and dissolution rate as a function of acidity, with Nd^{3+} present.

Table 14: Calculated dissolution rate and solubility limit in the presence of roughly 80 mM Nd^{3+} as a function of HNO_3 concentration.

$[HNO_3]$ M	k (g/cm^2 d)	$[Bi]_{Eq}$ (mM)
4.3	170 ± 10	660 ± 30
5.0	160 ± 10	950 ± 50
6.0	260 ± 10	1200 ± 100

Next sodium bismuthate's dissolution was observed in nitric acid with Zr^{4+} present in a similar manner as the previous ions. This first experiment was performed with a varying $[Zr^{4+}]$, with a constant acidity, as shown in Figure 25. Table 15 displays the calculated rate of dissolution and solubility limit of sodium bismuthate. The rate decreases linearly with an increase in $[Zr^{4+}]$. Despite this decrease, the rate was still

notably larger than what is observed in acid-only system, even in the highest concentration of Zr^{4+} observed. This increase in rate with the presence of Zr is likely due to the use of $ZrOCl_2$ starting material. The chloride ions which dissolve into solution can be oxidized by bismuthate, generating Cl_2. This is in line with what was observed, as significant gas formation occurred upon contacting the sodium bismuthate powder with the zirconyl chloride solution, resulting in an aroma of a chlorinated swimming pool. The presence of Cl^- creates a new redox pathway for bismuthate improving its dissolution kinetics. An indirect correlation was observed between sodium bismuthate's solubility limit and $[Zr^{4+}]$, with a reduction of roughly 40%, when Zr^{4+} was present at 230 mM. This, much like Nd^{3+}, is attributed to the common ion effect.

When the Zr^{4+} concentration was held constant at roughly 50 mM, the solubility limit was seen to increase with an increasing acidity (see Figure 28). The presence of Zr^{4+} improved the rate of dissolution in comparison to the nitric acid-only studies. However, increasing the acidity appeared to have little effect on the rate. When the acidity was set to 5.0 M, the data deviates from the inverse cubic fit. This is believed to be caused by a sampling error. The solubility limit of the sodium bismuthate was progressively diminished in 4.3, 5.0, and 6.0 M nitric acid, by approximately 10%, 22%, and 40%, respectively, versus the acid only systems. It can be seen from these experiments that Zr^{4+} has a sizeable effect on the dissolution of sodium bismuthate and might be an issue for the oxidation of the actinides, however, due to chloride's oxidation in this system, these results are not necessarily definitive.

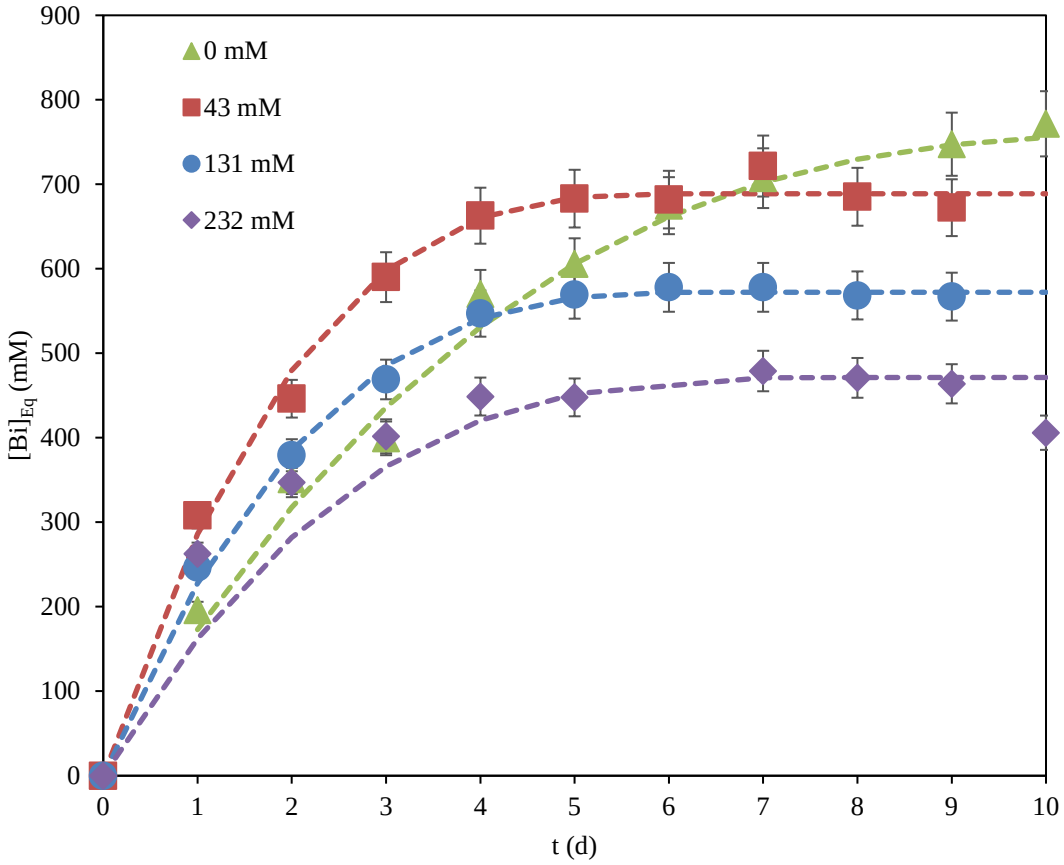

Figure 25: Dissolution of sodium bismuthate in 4.3M HNO_3 over ten days, with Zr^{4+} present.

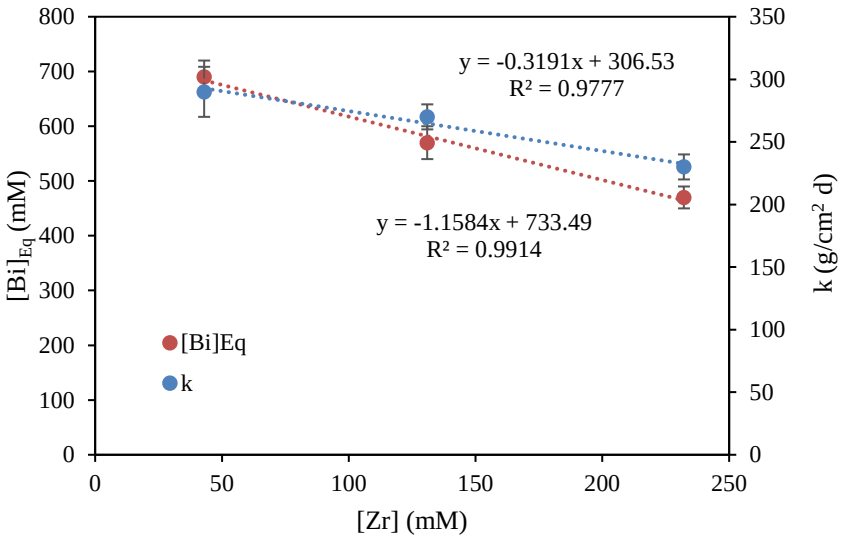

Figure 26: Solubility limit and dissolution rate of sodium bismuthate as a function of Zr^{4+} concentration.

Table 15: Calculated dissolution rate and solubility limit in 4.3 M HNO_3 as a function of Zr^{4+} concentration.

$[Zr^{4+}]$ (mM)	k (g/cm^2 d)	$[Bi]_{Eq}$ (mM)
0	150 ± 10	760 ± 40
43	290 ± 20	690 ± 30
130	270 ± 10	570 ± 30
230	230 ± 10	470 ± 20

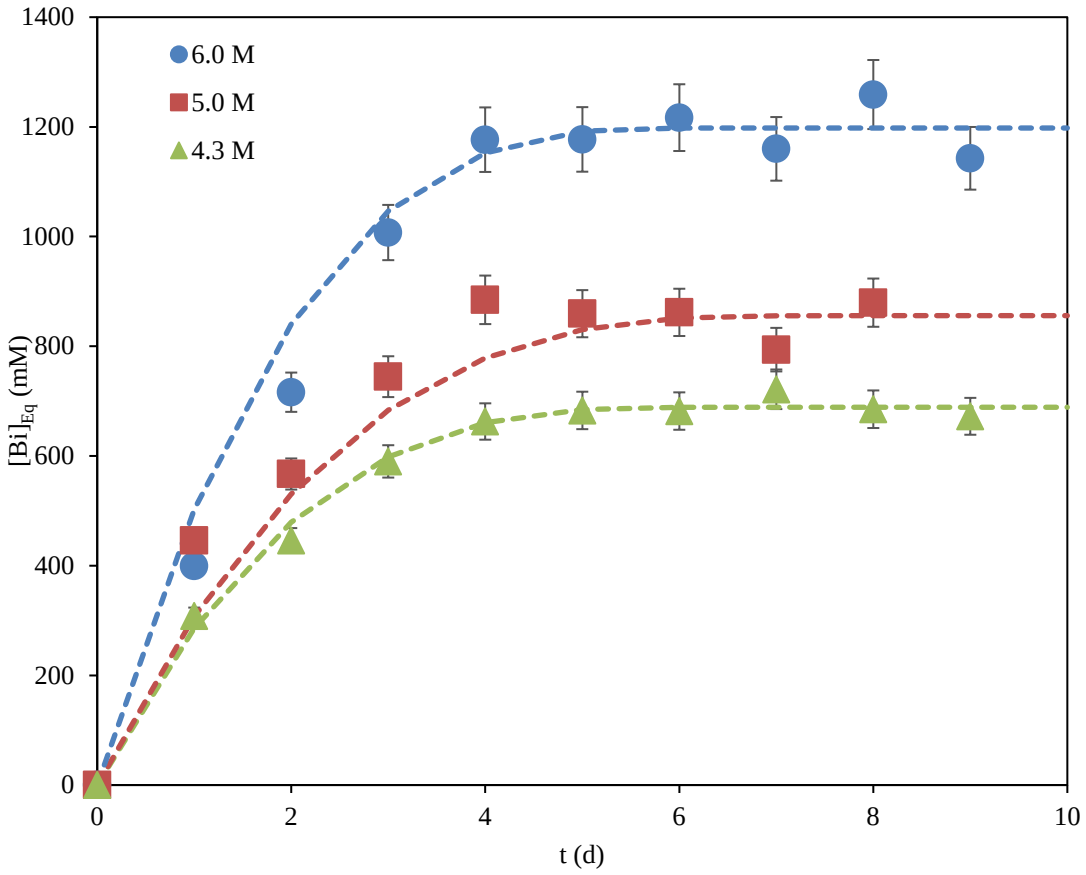

Figure 27: Dissolution of sodium bismuthate in 4.3, 5.0, and 6.0 M HNO_3 over ten days, with Zr^{4+} present.

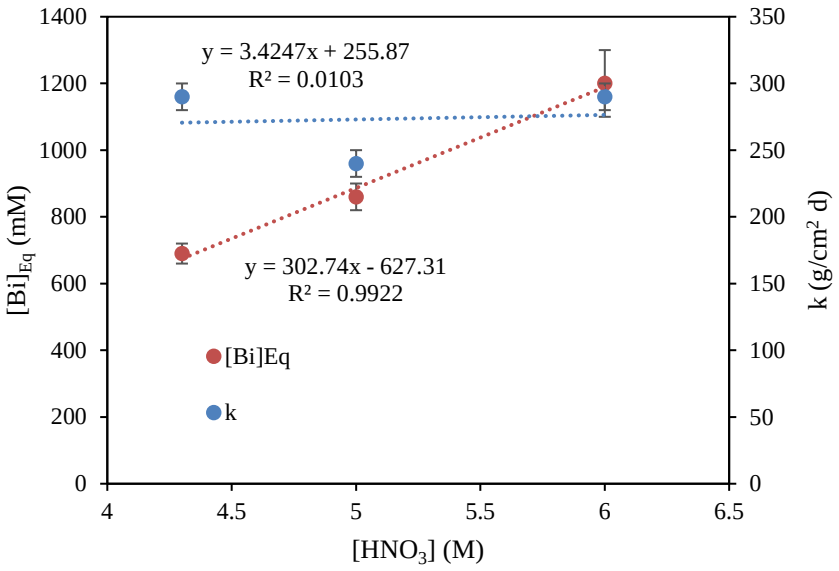

Figure 28: Solubility limit and dissolution rate as a function of acidity, with Zr^{4+} present.

Table 16: Calculated dissolution rate and solubility limit in the presence of roughly 50 mM Zr^{4+} as a function of HNO_3 concentration.

$[HNO_3]$ (M)	k (g/cm^2 d)	$[Bi]_{Eq}$ (mM)
4.3	290 ± 10	690 ± 30
5.0	240 ± 10	860 ± 40
6.0	290 ± 10	1200 ± 100

Cerium was then chosen for investigation to determine how a redox active ion would affect the dissolution of sodium bismuthate. These studies were performed as previously detailed with Cs^+. Figure 29 shows the results of varying the total Ce

concentration, while holding the acid constant at 4.3 M HNO_3. It can be seen in Table 17 that the rate of bismuthate dissolution was significantly increased when the cerium concentration was increased. This improvement in rate is likely due to a second pathway available for the dissolution of sodium bismuthate, as described in Equation 3. However, the 50% decrease in solubility limit of Bi between no cerium present and 162 mM [Ce] is likely due to the presence of Ce^{3+} in solution, which reduces the production of Bi^{3+} due to similar ionic behavior between these two ions.

When the the total Ce concentration was held constant at roughly 44 mM, the solubility limit of sodium bismuthate was seen to increase linearly as a function of acidity (see Figure 32). Much like when Zr^{4+} was present, the solubility limit progressively diminishes by roughly 11%, 27%, and 45% at the acidity increase from 4.3 M to 5.0 and 6.0 M HNO_3, respectively. There appears to be an indirect correlation between the dissolution rate of sodium bismuthate and increasing acidity shown in Figure 32, however the trend is not definitive as the *k* values found in the 4.3 and 5.0 M nitric acid systems could be the same due to their uncertainties. Regardless of this trend, all three rates are still significantly larger than the ones found in the nitric acid only tests. These cerium studies illustrate that it is not desirable to have large quantities of cerium present in solution when the oxidation of U through Am is performed, while the sodium bismuthate's slow dissolution kinetics are improved, it is most likely due to the oxidation of Ce^{3+} to Ce^{4+}, an undesirable consumption of the BiO_3^-.

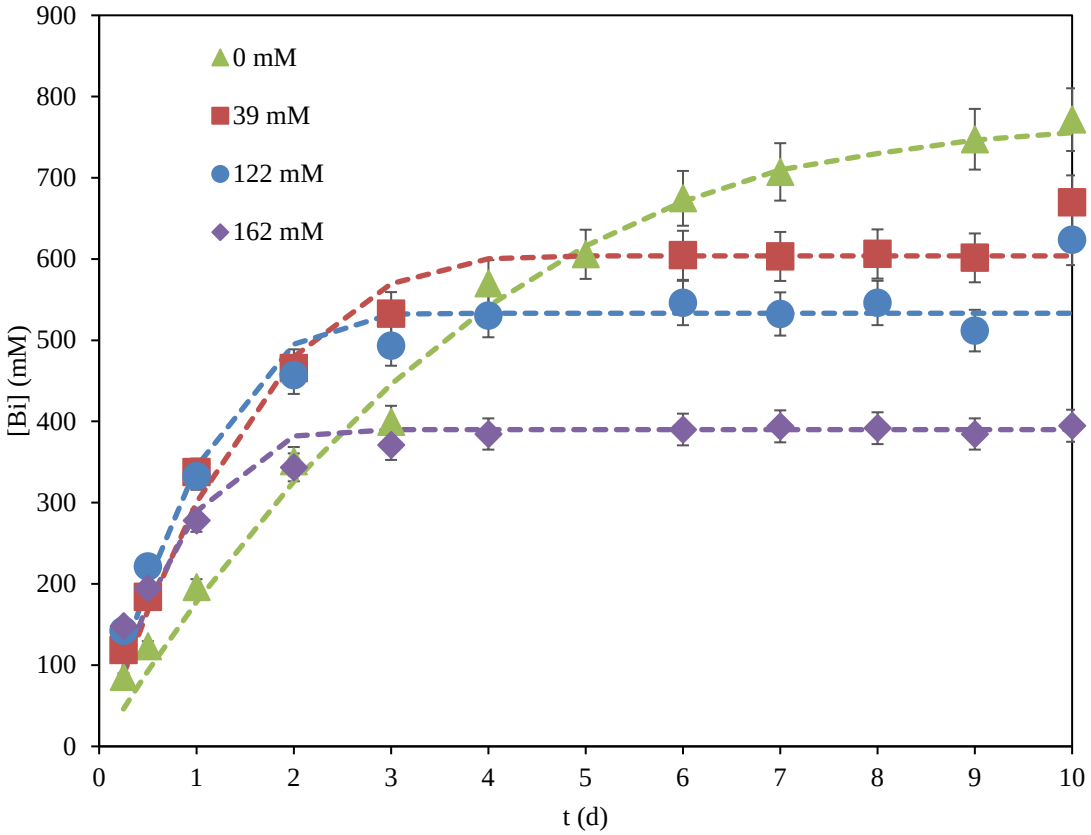

Figure 29: Dissolution of sodium bismuthate in 4.3 M HNO_3 over ten days, with $Ce^{3+/4+}$ present.

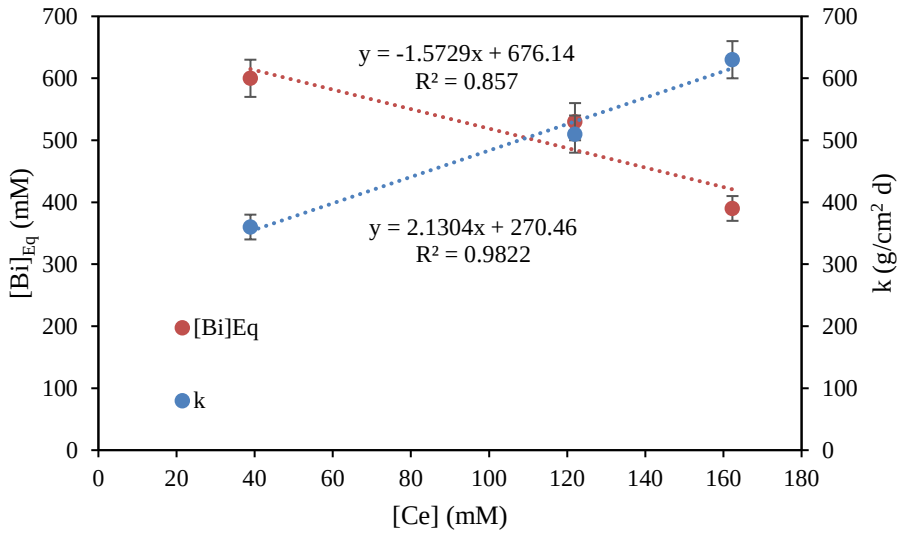

Figure 30: Solubility limit and dissolution rate of sodium bismuthate as a function of $Ce^{3+/4+}$ concentration.

Table 17: Calculated dissolution rate and solubility limit in 4.3 M HNO_3 as a function of $Ce^{3+/4+}$ concentration.

[Ce] (mM)	k (g/cm^2 d)	$[Bi]_{Eq}$ (mM)
0	150 ± 10	760 ± 40
39	360 ± 20	600 ± 30
120	510 ± 30	530 ± 30
160	630 ± 30	390 ± 20

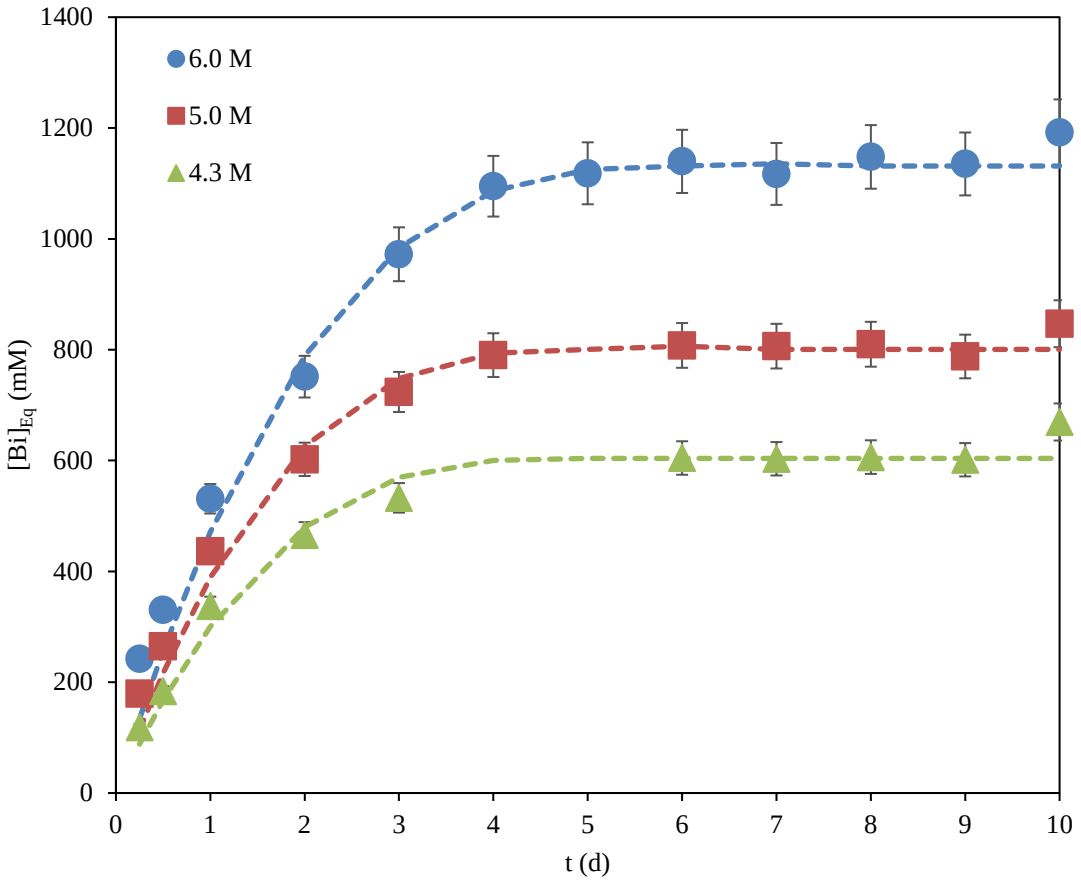

Figure 31: Dissolution of sodium bismuthate in 4.3, 5.0, and 6.0 M HNO_3 over ten days, with $Ce^{3+/4+}$ present.

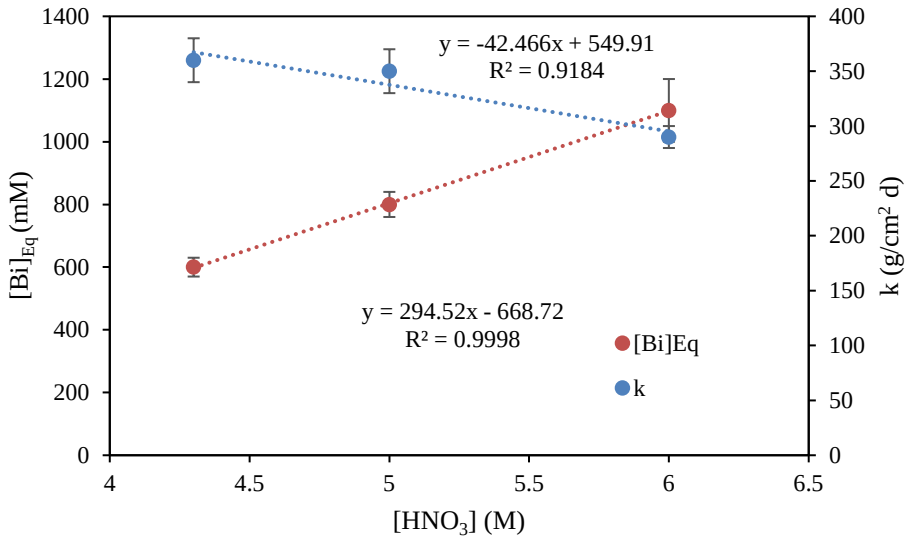

Figure 32: Solubility limit and dissolution rate as a function of acidity, with $Ce^{3+/4+}$ present.

Table 18: Calculated dissolution rate and solubility limit in the presence of roughly 40 mM $Ce^{3+/4+}$ as a function of HNO_3 concentration.

$[HNO_3]$ (M)	k (g/cm^2 d)	$[Bi]_{Eq}$ (mM)
4.3	360 ± 20	600 ± 30
5.0	350 ± 20	800 ±40
6.0	290 ± 10	1100 ± 100

Finally, a study was performed to determine how the presence of U affects the dissolution of $NaBiO_3$ in HNO_3, since uranium makes up a large percentage of UNF. In this experiment the nitric acid concentration was held constant at 4.3 M, and the concentration of U was varied (see Figure 33). As can be seen from Table 19 and Figure 34, the increase of U seems to correlate to increase the rate of dissolution and the solubility of sodium bismuthate in nitric acid. It is difficult, however, to come to a

conclusion about how these two ions are interacting in solution since there was a decrease in the solubility limit from 0-50 mM [U] present, and then an increase in these values when the [U] was increased to 132 and 209 mM. More investigation should be done with respect to the interaction between these two ions to determine how uranium would affect this process, as these data are inconclusive.

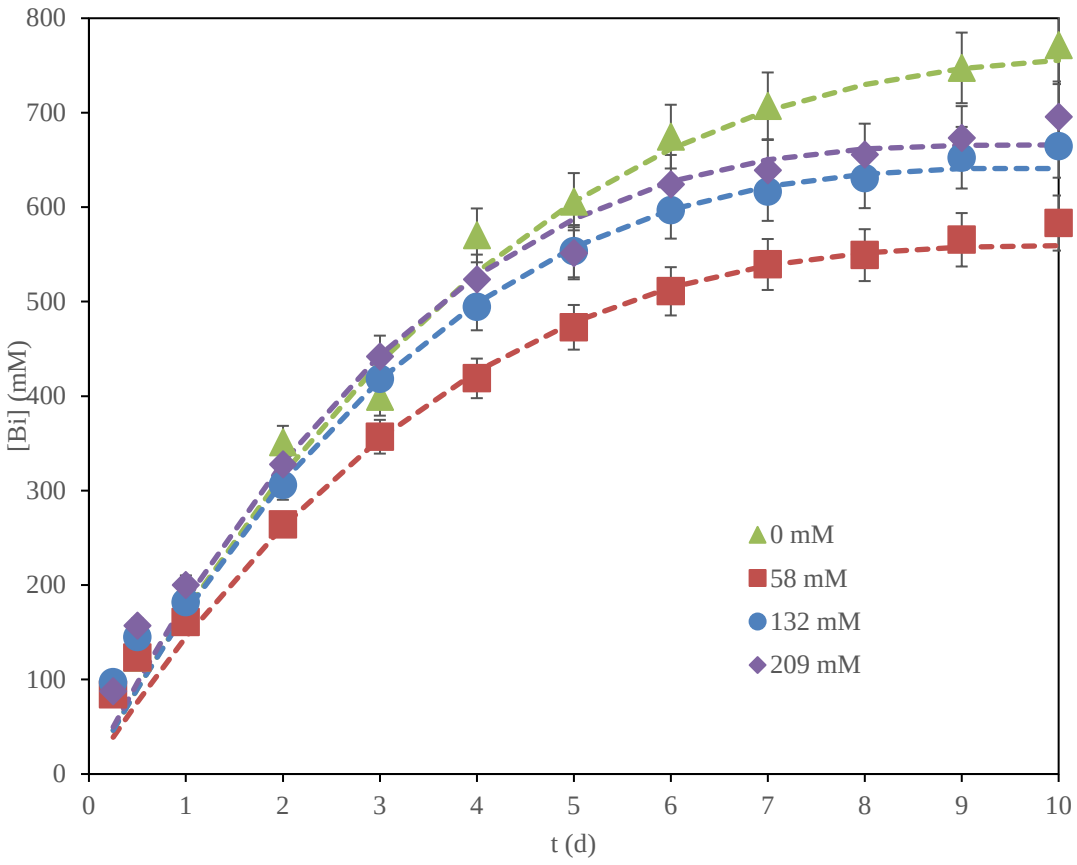

Figure 33: Dissolution of sodium bismuthate in 4.3 M HNO_3 over ten days, with UO_2^{2+} present.

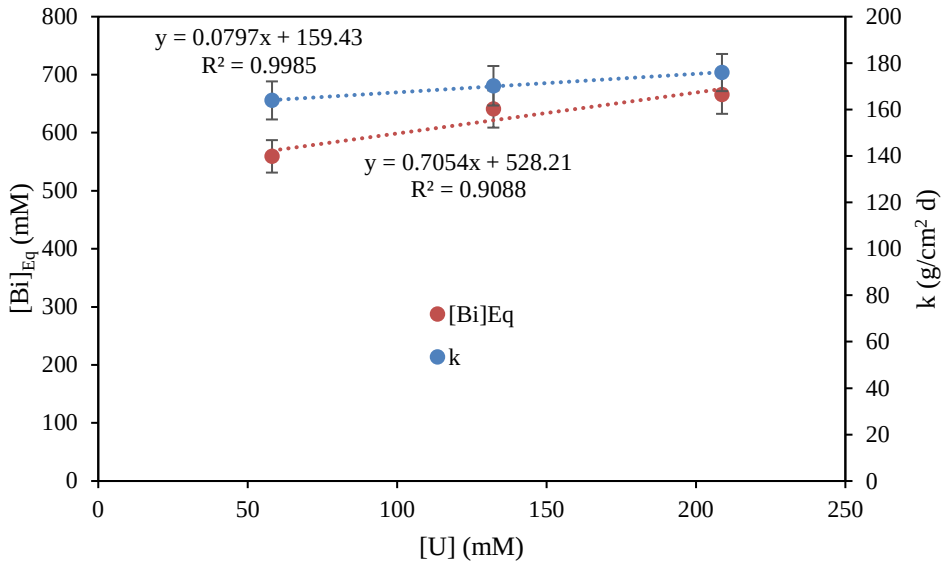

Figure 34: Solubility limit and dissolution rate of sodium bismuthate as a function of UO_2^{2+} concentration.

Table 19: Calculated dissolution rate and solubility limit in 4.3 M HNO_3 as a function of UO_2^{2+} concentration.

[U] (mM)	k (g/cm^2 d)	$[Bi]_{Eq}$ (mM)
0	150 ± 10	760 ± 40
58	170 ± 10	560 ± 30
130	170 ± 10	640 ± 30
210	180 ± 10	660 ± 30

To gain a better understanding how each ion affected the dissolution if sodium bismuthate and any differences, the results for similar studies were plotted in single figures. Figure 35 shows the differences of the dissolution of sodium bismuthate in 4.3 M HNO_3 with approximately 50 mM concentration of each of the ions studied, along with the acid-only system. It is obvious, that cesium is a significant problem for the

dissolution of sodium bismuthate in 4.3 M HNO_3, as its behavior is strikingly inhibited compared to the other ions studied. Again this is likely due to Cs^+ replacing Na^+ and reducing the solubility of this $CsBiO_3$ ion before bismuthate can dissolve. UO_2^{2+} appears to have the second most negative effect on solubility limit, reducing bismuthates solubility to 560 mM [Bi]. Nd^{3+}, Zr^{4+}, and $Ce^{3+/4+}$ result in a slight lowering of the solubility of sodium bismuthate, most likely a result of these ions behaving similarly in solution which reduces the production of Bi^{3+}. Sr^{2+} has no effect on the solubility limit of bismuthate and improve the dissolution kinetics by almost 30%, in comparison to the acid-only system, which is likely due to its lack of interaction with bismuthate.

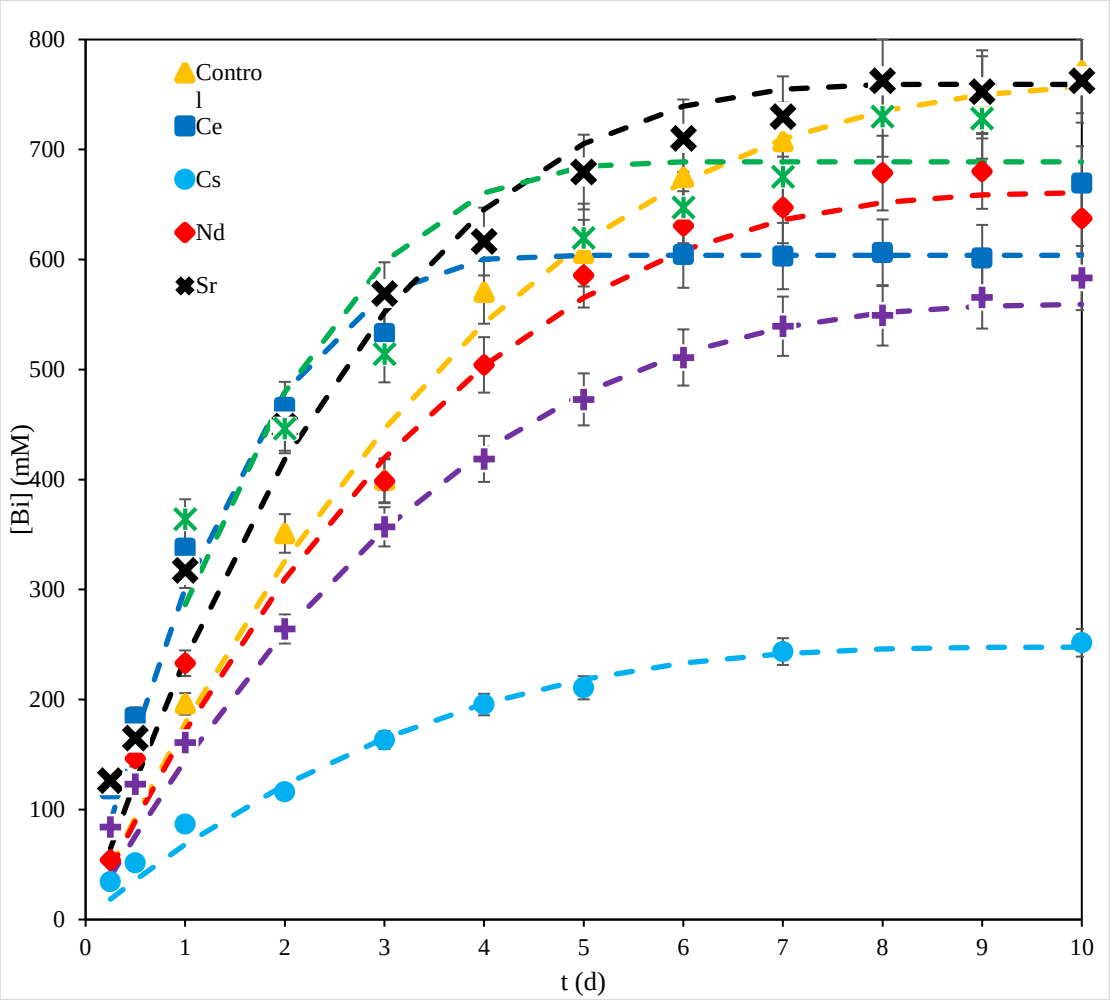

Figure 35: Comparison of the dissolution of sodium bismuthate in 4.3 M HNO_3 over ten days, with the ions UO_2^{2+}, Cs^+, Sr^{2+}, Nd^{3+}, Zr^{4+}, and $Ce^{3+/4+}$ present at roughly 50 mM.

In Figure 36, a comparison of the dissolution behavior of sodium bismuthate in 5.0 M HNO_3 can be seen. It appears the higher acidity improves the solubility and dissolution rates for each system. In fact, the negative effects of Cs^+ were significantly reduced and is similar with other fission products present. Again it can be seen that the presence of Sr^{2+} exhibits only minor effects on the solubility of bismuthate. The

solubility of sodium bismuthate in the Nd^{3+}, Zr^{4+}, and $Ce^{3+/4+}$ experiments was improved in this higher acidity.

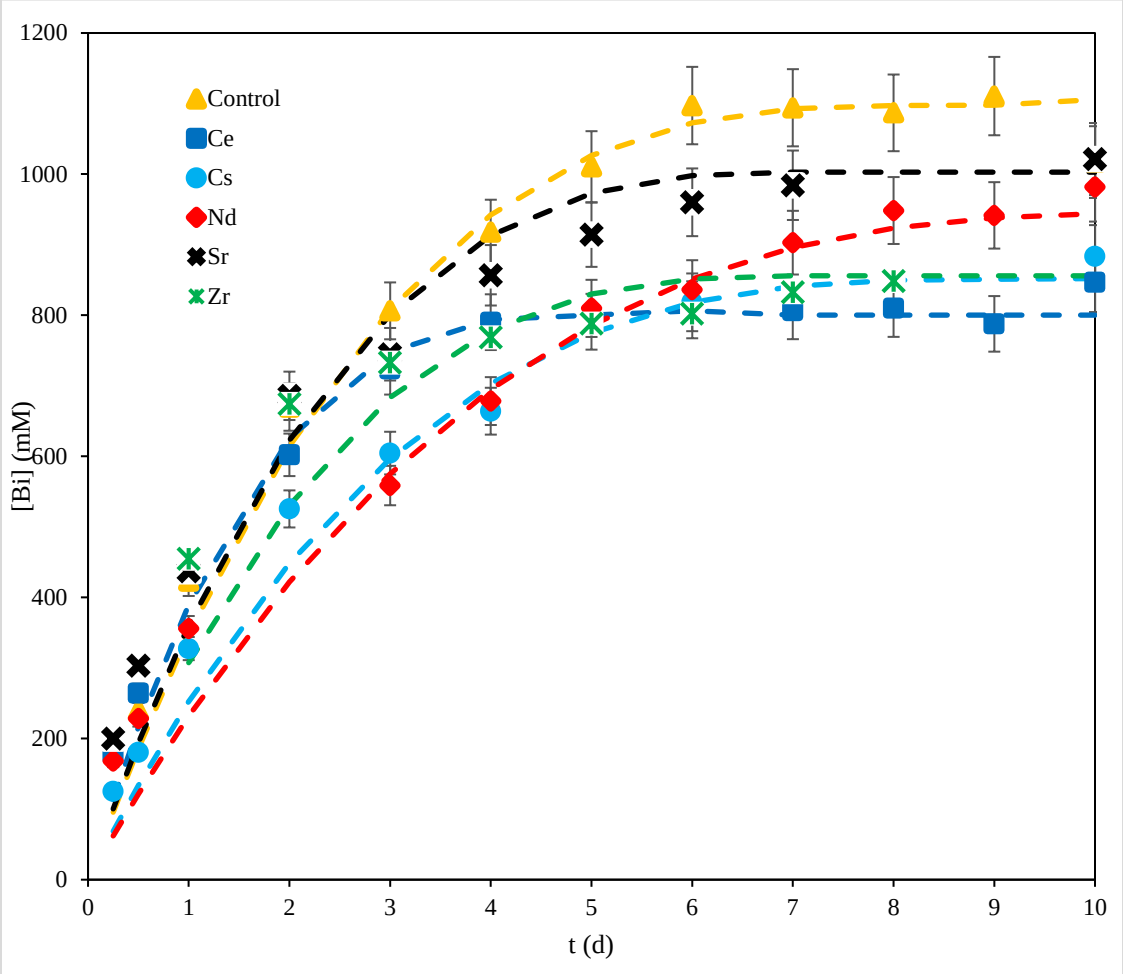

Figure 36: Comparison of the dissolution of bismuthate in 5.0 M HNO_3 over a period of ten days, with the ions Cs^{+}, Sr^{2+}, Nd^{3+}, Zr^{4+}, and $Ce^{3+/4+}$ present.

Finally, a comparison in 6.0 M HNO_3 can be seen in Figure 37. There appears to be diminishing returns for the dissolution characteristics by significantly increasing the acidity for for Cs^{+}, Nd^{3+}, Zr^{4+}, and $Ce^{3+/4+}$ present. The solubility of sodium bismuthate

in each study appeared to converge to approximately 1100 mM [Bi]. However, the solubility of sodium bismuthate with Sr^{2+} present seemed to be only slightly affected, and was much more in line with the acid-only system.

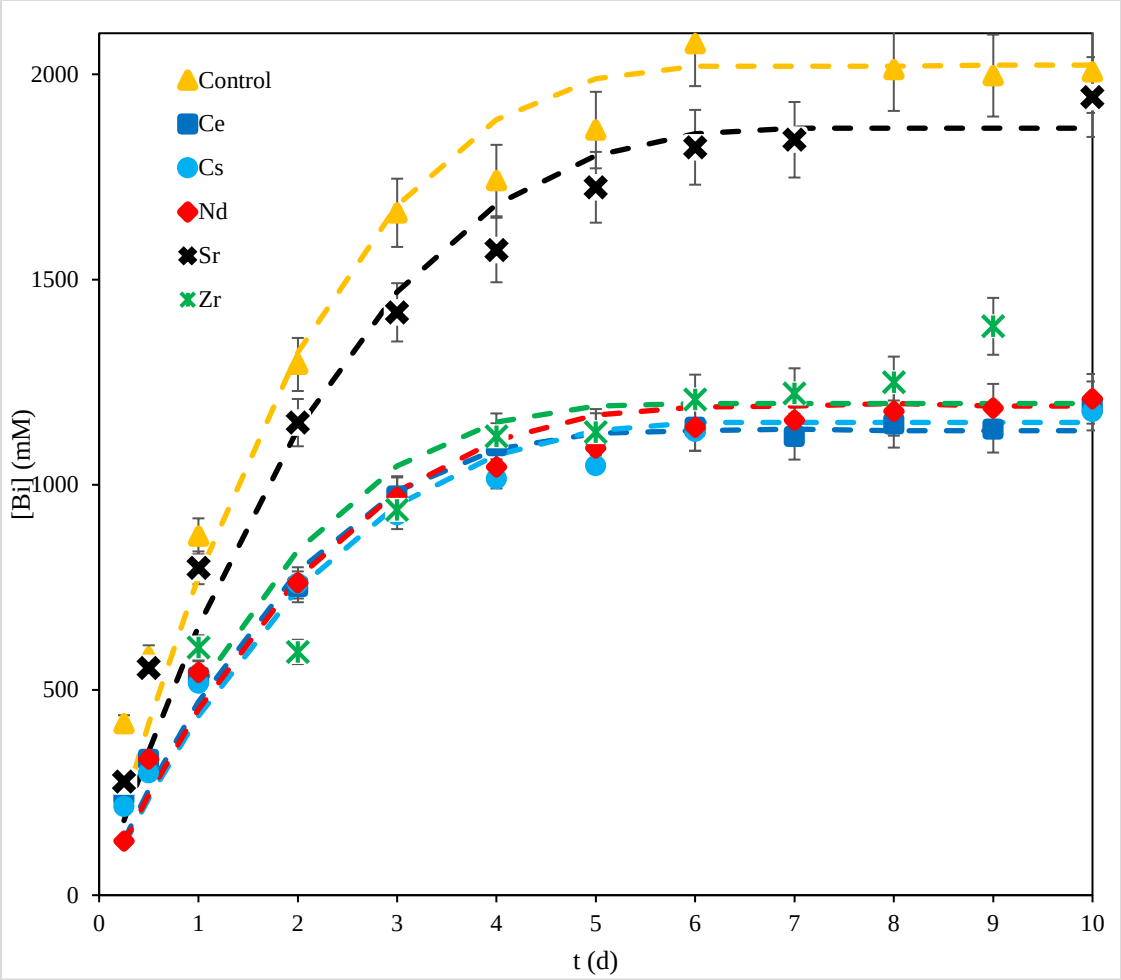

Figure 37: Comparison of the dissolution of bismuthate in 6.0 M HNO_3 over a period of ten days, with the ions Cs^{+}, Sr^{2+}, Nd^{3+}, Zr^{4+}, and Ce^{3+} and $Ce^{3+/4+}$ present.

Overall, these result show that the behavior of sodium bismuthate is influenced by presence of other metal ions in solution. Some ions, like with Sr^{2+}, have little effect on the dissolution, while others, Cs^{+} for example, which is present in relatively large quantities, have a profound effect on the system. If a process were to be designed using sodium bismuthate as an oxidant, careful attention would have to be given to those species that affect the system significantly, to ensure the desired goal could be achieved.

4. CONCLUSIONS AND FUTURE WORK

The importance of closing the nuclear fuel cycle and the necessity for UNF recycle options has been expressed in this thesis. It was explained that $NaBiO_3$ could potentially play an integral role in separating recyclable actinides from fission products and other remaining waste, reducing the heat load on nuclear fuel repositories, drastically reducing the length of time needed for storage of this waste. To better understand the properties of sodium bismuthate and how well it would suit a UNF separation process as an oxidizing agent, the solubility limit and dissolution kinetics were measured in nitric acid. Secondary ions, key stable fission product surrogates and uranium, were added to the system in varying concentrations and their effects were studied. In a control experiment with no secondary ions present and in varying acidity, the rate of dissolution of bismuth was observed in a range from 150-260 g cm^{-2} d^{-1}, and the solubility was observed in a range from 760-2000 mM [Bi]. When cerium and neodymium were added to the system the solubility limit was reduced to about 400-1200 mM [Bi], in both cases. The cerium improved the dissolution kinetics of bismuth, increasing the rate of dissolution to a range of 860-630 g cm^{-2} d^{-1}, while the kinetics remained about the same in the presence of Nd^{3+}. Cesium had a significant effect on bismuthate's dissolution by decreasing its solubility limit to a range of 84-1200 mM [Bi], while it seemed to have a negligible effect on the rate of dissolution of bismuthate, as the *k* values of this experiment matched those of the control experiment. The lower concentrations of strontium had a negligible effect on the rate of dissolution and

solubility limit of [Bi], as these values were found to be very similar to those found in the control experiments. However, in an experiment where about 260 mM [Sr^{2+}] was present, the solubility limit of bismuthate was slightly reduced. Zr^{4+} also reduced the solubility limit of bismuth to a range of 470-1200 mM, while the rate of dissolution was moderately improved. The presence of Zr also improved the dissolution rate values to a range of 230-290 g cm^{-2} d^{-1}. Nd and Zr have some effect on the solubility limit of bismuth it a large solution due to varying degrees of the common ion effect, and appear to improve bismuth's rate of dissolution. These ions might have a small impact a large scale oxidation process, using bismuthate as the oxidizing agent, and their impact must be assessed with the requirements of the process in mind. In the case of cesium, it is believed that this ion replaces Na^{+} and prevents bismuthate from ever significantly dissolving due to a reduction in solubility. This could be an issue for incorporating bismuthate as an oxidizing agent in recycle processes, as cesium makes up a large portion of the fission products present in UNF. Ce^{3+} could also be a significant issue for a large scale process which employs bismuthate as an oxidizing agent. This ion improves dissolution kinetics by causing BiO_3^- to reduce to Bi^{3+}, however this redox reaction consumes bismuthate, which means there would be less of this oxidizing agent available to oxidize the actinides. Sr^{2+} had almost no effect on the dissolution behavior of bismuthate and appeared to not interact with bismuthate at all.

U was also added to the system to determine how this actinide might affect bismuthate's dissolution, since it makes up a large portion of UNF. The presence of

uranium in solution seemed to have a small effect on the change in the rate of dissolution of Bi with values ranging from 170-180 g cm^{-2} s^{-1}. More investigation must be done on uranium's impact on the solubility limit of bismuth to make a coherent conclusion. This is because the presence of uranium decreased the solubility limit of bismuth, however when the uranium concentration was increased, the solubility limit was found to increase as well.

In a continuing investigation of bismuthate, it would be interesting to determine if there is any complexation or other interactions taking place in the presence of these secondary ions. In this analysis the dissolution of the total bismuthate concentration was measured and analyzed, however it would be helpful to measure the Bi^{3+} production rate and bismuthate reduction rate. It would be interesting to further investigate the effect $NaBiO_3$ has on the co-crystallization of the minor actinides.[26]

REFERENCES

1. D. Goodstein, *Out of Gas-The End of the Age of Oil*, Norton & Company, New York City, (2005).

2. K. L. Nash, G. J. Lumetta, S. B. Clark, & J. Friese “Significance of the Nuclear Fuel Cycle in the 21 st Century;” https://doi.org/10.1021/bk-2006-0933.ch001.

3. R. C. Ewing, “The Nuclear Fuel Cycle versus The Carbon Cycle,” Can. Mineral. 43 6, 2099 (2005); https://doi.org/10.2113/gscanmin.43.6.2099.

4. L. Gagnon, C. Belanger, and Y. Uchiyama, “Life-cycle assessment of electricity generation options: The status of research in year 2001,” 30 (2002) 1267-1278. Energy Policy (2002). https://doi.org/10.1016/S0301-4215(02)00088-5

5. “Updated EIA survey provides data on spent nuclear fuel in the United States - Today in Energy - U.S. Energy Information Administration (EIA);” (2012). Retrieved August 16, 2017, from https://www.eia.gov/todayinenergy/detail.php?id=24052.

6. O. US EPA, “Summary of the Nuclear Waste Policy Act.” (2008) Retrieved August 17, 2017 from https://www.epa.gov/laws-regulations/summary-nuclear-waste-policy-act

7. On-Site Storage of Nuclear Waste - Nuclear Energy Institute. (n.d.). Retrieved August 16, 2017, from https://www.nei.org/Knowledge-Center/Nuclear-Statistics/On-Site-Storage-of-Nuclear-Waste

8. T. M. Ahn, S. Mohanty, "Dissolution Kinetics of Commercial Spent Nuclear Fuels in the Potential Yucca Mountain Repository Environment" Office of Nuclear Material Safety and Safeguards (2008). Retrieved August 17, 2017 from https://www.nrc.gov/docs/ML0831/ML083120074.pdf

9. W. E. Lee, “Chapter 11: Long-Lived Waste Radionuclides | Engineering360,” Copyright Elsevier Ltd.; 2005; https://www.globalspec.com/reference/36859/203279/chapter-11-long-lived-waste-radionuclides; (current as of Feb. 20, 2018).

10. “NRC: Backgrounder on Radioactive Waste;” (2017). Retrieved August 22, 2017, from https://www.nrc.gov/reading-rm/doc-collections/fact-sheets/radwaste.html.

11. R. Taylor, *Reprocessing and Recycling of Spent Nuclear Fuel*, Part 1 Chapter 1 p. 3-23, Elsevier Science Technology, United Kingdom (2015); https://doi.org/10.1016/C2013-0-16483-5.

12. M. Salvatores, “Nuclear fuel cycle strategies including Partitioning and Transmutation,” Nucl. Eng. Des. 235, 805 (2005); https://doi.org/10.1016/j.nucengdes.2004.10.009.

13. D. Čalic, “Nuclear Energy for New Europe 2005 Waste Management In Future Partioning And Transmutation (P&T).” Presented at Nuclear Energy for New Europe 2005. Bled, Slovenia. Retrieved August 18, 2017 from http://www.djs.si/proc/bled2005/htm/pdf/0177.pdf

14. T. Suzuki et al., “Separation of americium and curium by use of tertiary pyridine resin in nitric acid/methanol mixed solvent system,” in Journal of Radioanalytical and Nuclear Chemistry 272 2, pp. 257–262 (2007); https://doi.org/10.1007/s10967-007-0511-8.

15. B. J. Mincher, G. Modolo, and S. P. Mezyk, “Review: Solvent Extraction and Ion Exchange Review: The Effects of Radiation Chemistry on Solvent Extraction 4: Separation of the Trivalent Actinides and Considerations for Radiation- Resistant Solvent Systems” 28, 415-456, (2018); https://doi.org/10.1080/07366299.2010.485548.

16. Ahn, J. (2010). "Assessment of Partitioning Processes for Transmutation of Actinides". IAEA-TECDOC-1648 Retrieved August 20, 2017 from http://www-pub.iaea.org/MTCD/Publications/PDF/TE_1648_CD/PDF/TECDOC_1648.pdf

17. J. Veliscek-Carolan, “Separation of actinides from spent nuclear fuel: A review,” J. Hazard. Mater. 318, 266 (2016); https://doi.org/10.1016/j.jhazmat.2016.07.027.

18. E. Philip Horwitz, D. C. Kalina, H. Diamond, G. F. Vandegrift, & W. W. Schulz, “The TRUEX Process - A Process For The Extraction Of The Transuranic Elements From Nitric Acid in Wastes Utilizing Modified Purex Solvent*,” Solvent Extr. Ion Exch. 3 1–2, 75, (1985); https://doi.org/10.1080/07366298508918504.

19. K. L. Nash and G. R. Choppin, “Separations Chemistry for Actinide Elements: Recent Developments and Historical Perspective,” Sep. Sci. Technol. 32 1–4, 255 (1997); https://doi.org/10.1080/01496399708003198.

20. S. Chapron, C. Marie, G. Arrachart, M. Miguirditchian, & S. Pellet-Rostaing, “New Insight into the Americium/Curium Separation by Solvent Extraction using Diglycolamides,” Solvent Extr. Ion Exch. 33 3, 236 (2015); https://doi.org/10.1080/07366299.2014.1000792.

21. J. M. Richards and R. Sudowe, “Separation of Americium in High Oxidation

States from Curium Utilizing Sodium Bismuthate;" Anal. Chem. 88 (9), 4605-4608, (2016); https://doi.org/10.1021/acs.analchem.6b01026.

22. J. D. Burns et al., "Separation of Americium from Curium by oxidation and ion exchange," Anal. Chem. 84 16, 6930 (2012); https://doi.org/10.1021/ac3018394.

23. K. L. Nash and G. J. Lumetta, *Advanced separation techniques for nuclear fuel reprocessing and radioactive waste treatment*, Woodhead Publishing (2011); Retrieved August 15, 2017 from https://books.google.com/books?hl=en&lr=&id=z4xwAgAAQBAJ&oi=fnd&pg=PA377&dq=Solid-phase+extraction+technology+for+actinide+and+lanthanide+separations+in+nuclear+fuel+reprocessing&ots=yhWYs8jSs5&sig=t9xI_JhNfuPFVdW7lN0PurJ6Bj4#v=onepage&q=Solid-phase extraction technology for actinide and lanthanide separations in nuclear fuel reprocessing&f=false.

24. T. Inoue and L. Koch, "Development of Pyroprocessing and its Future Direction," Nucl. Eng. Technol. 40 3 (2008). Retrieved September 18, 2017 from https://kns.org/jknsfile/v40/JK0400183.pdf

25. K. Ikeda, S. I. Koyama, M. Kurata, Y. Morita, K. Tsujimoto, & K. Minato, "Technology readiness assessment of partitioning and transmutation in Japan and issues toward closed fuel cycle," Prog. Nucl. Energy 74, 242 (2014); https://doi.org/10.1016/j.pnucene.2013.12.009.

26. J. D. Burns and B. A. Moyer, "Group Hexavalent Actinide Separations: A New Approach to Used Nuclear Fuel Recycling," Inorg. Chem. 55 17, 8913 (2016); https://doi.org/10.1021/acs.inorgchem.6b01430.

27. T. CHIKAZAWA et al., "Batch Crystallization of Uranyl Nitrate," J. Nucl. Sci. Technol. 45 6, 582 (2008); https://doi.org/10.1080/18811248.2008.9711882.

28. M. Nakahara, Y. Nakajima, and T. Koizumi, "Washing of uranyl nitrate hexahydrate crystals with nitric acid aqueous solution to improve crystal quality," Ind. Eng. Chem. Res. 51 46, 15170 (2012); https://doi.org/10.1021/ie3013067.

29. Y. Sano et al., "Plutonium and other actinides behaviour in NEXT process," J. Alloys Compd. 444–445 SPEC. ISS., 397 (2007); https://doi.org/10.1016/j.jallcom.2007.03.092.

30. M. Nakahara, T. Koizumi, and K. Nomura, "Behavior of Actinide Elements and Fission Products in Recovery of Uranyl Nitrate Hexahydrate Crystal by Cooling Crystallization Method," Nucl. Technol. 174 1, 109 (2011); https://doi.org/https://doi.org/10.13182/NT11-A11684.

31. B. J. Mincher, L. R. Marting, and N. C. Scmitt, “Tributylphosphate Extraction Behavior of Bismuthate-Oxidized Americium” Inorg. Chem. 47 15, 6984-6989 (2008); https://doi.org/10.1021/ic800667h.

32. A. Mills and X. Li, “Kinetics of reductive dissolution of sodium bismuthate by CeIII and MnII ions,” J. Chem. Soc. Faraday Trans. 90 19, 2939 (1994); https://doi.org/10.1039/FT9949002939.

33. D. Shriver, P. W. Atkins *Inorganic Chemistry* 3d ed. Chap. 2 p. 61-62, W. H. Freeman and Company, New York, (1999).